Cohesive Models of Fracture

Michael Ortiz

Caltech

Solid Mechanics at the turn of the Millennium

Providence, RI, June16, 2000

Introduction

- Cohesive theories of fracture are phenomenological continuum theories characterized by two independent constitutive descriptions:
  - *A constitutive law governing the deformation in the bulk.*
  - *A cohesive law governing separation across cohesive surfaces.*
- The cohesive constitutive law embodies a description of the mechanical effects of the separation processes and the dissipation associated with them.
- Origins in work of Dugdale (1960) and Barrenblatt (1962). Equivalence to Griffith's criterion shown by Willis (1967) and Rice (1968).

Introduction (cont'd)

- Cohesive theories of fracture provide a means of addressing certain issues that are difficult to address within classical fracture mechanics, including:
  - *Nucleation in solids with no discernable initial flaws*
  - *Tracking of tortuous crack paths*
  - *Profuse branching, fragmentation*
  - *Small cracks, fully yielded configurations*
  - *Effect of free surfaces, inhomogeneities, interfaces*
  - *Dynamic effects, crack-tip velocity*
  - *Arbitrary loading paths, unloading, overloads*

Introduction (cont'd)

- Cohesive theories of fracture provide a simple means of incorporating additional physics into the description of separation processes, including:
  - *Dislocation emission, interplanar potentials (Needleman, 1990; Beltz and Rice, 1991; Rice, 1992)*
  - *Friction after debonding (Tvergaard, 1990)*
  - *Chemistry, corrosion (Rice et al. 1976; Wang and Rice, 1989)*
  - *Closure (Hutchinson and Budiansky, 1978), hysteresis.*
- Cohesive theories of fracture enable the numerical simulation of processes and phenomena which are difficult to simulate within the framework of classical fracture mechanics (Hillerborg, 1976; Needleman, 1987)

Cohesive behavior

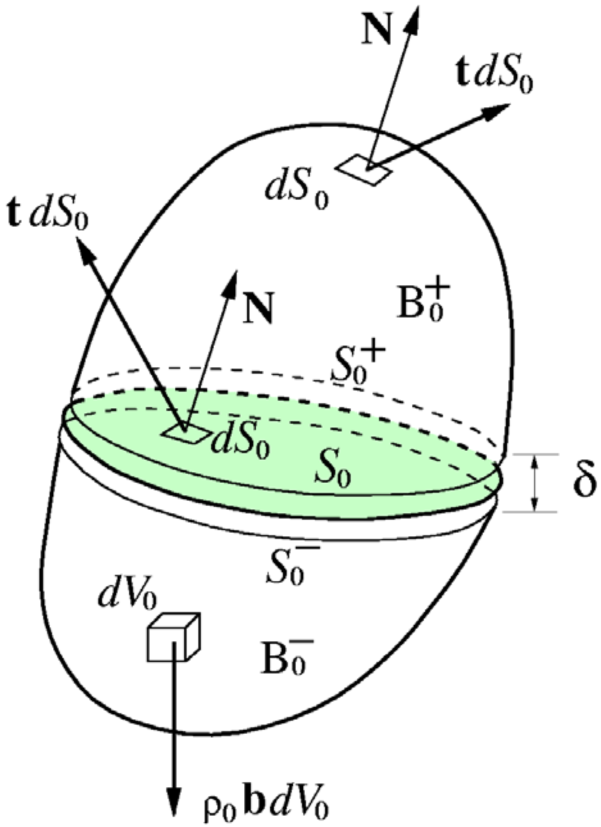

Schematic of body containing cohesive surface.
(Ortiz and Pandolfi, 1999)

- Deformation power identity:

$$P^D = \dot{W} - \dot{K} =$$

$$\sum_{\pm} \int_{B_0^\pm} \mathbf{P} \cdot \dot{\mathbf{F}} dV_0 + \int_{S_0} \mathbf{t} \cdot \dot{\boldsymbol{\delta}} dS_0$$

- Free energy/unit surface:

$$\phi(\mathbf{F}_p, \boldsymbol{\delta}, \theta, \mathbf{q}) = \epsilon A((\mathbf{F}_p | \boldsymbol{\delta}/\epsilon), \theta, \mathbf{q})$$

- Coleman's relations:

$$\mathbf{t} = \frac{\partial \phi}{\partial \boldsymbol{\delta}}(\mathbf{F}_p, \boldsymbol{\delta}, \theta, \mathbf{q})$$

- Kinetic relations:

$$\dot{\mathbf{q}} = \mathbf{f}(\mathbf{F}_p, \boldsymbol{\delta}, \theta, \mathbf{q})$$

Michael Ortiz

Cohesive behavior

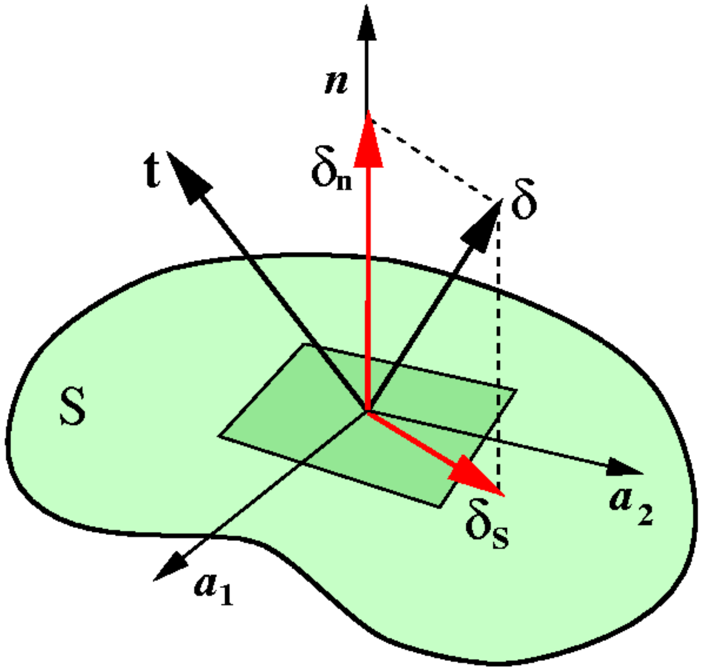

Local reference frame

- Material frame indifference:

$$\phi = \phi(\mathbf{C}_p, \boldsymbol{\delta} \cdot \mathbf{F}_p, \delta_n, \theta, \mathbf{q})$$

- Uncoupled stretching and opening:

$$\phi = \phi(\boldsymbol{\delta} \cdot \mathbf{F}_p, \delta_n, \theta, \mathbf{q})$$

- Isotropy:

$$\phi = \phi(\delta_s, \delta_n, \theta, \mathbf{q})$$

$$= \phi(\mathbf{n}, \boldsymbol{\delta}, \theta, \mathbf{q})$$

- Effective opening displacement (Tvergaard, 1990; Camacho and Ortiz, 1996):

$$\delta = \sqrt{\beta^2 \delta_s^2 + \delta_n^2}$$

$$\phi = \phi(\delta, \theta, \mathbf{q})$$

Michael Ortiz

Cohesive behavior

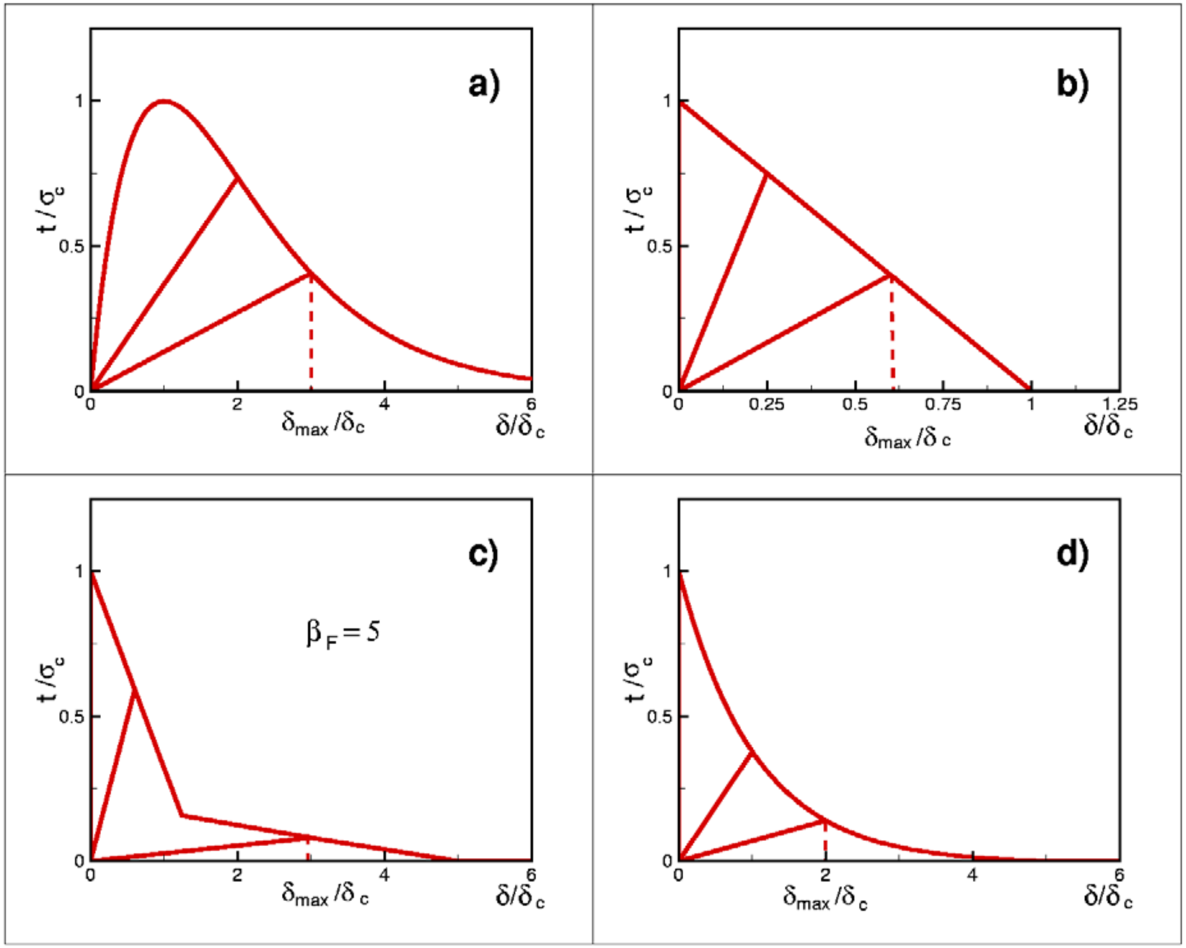

- Loading envelop:
  - *a) Rose-Ferrante*
  - *b) Linear*
  - *c) Bilinear*
  - *d) Exponential (Planas and Elices, 1990)*
- Loading/unloading irreversibility:
  - *Linear unloading to origin (Camacho and Ortiz, 1996)*

Michael Ortiz

Cohesive elements - 3D

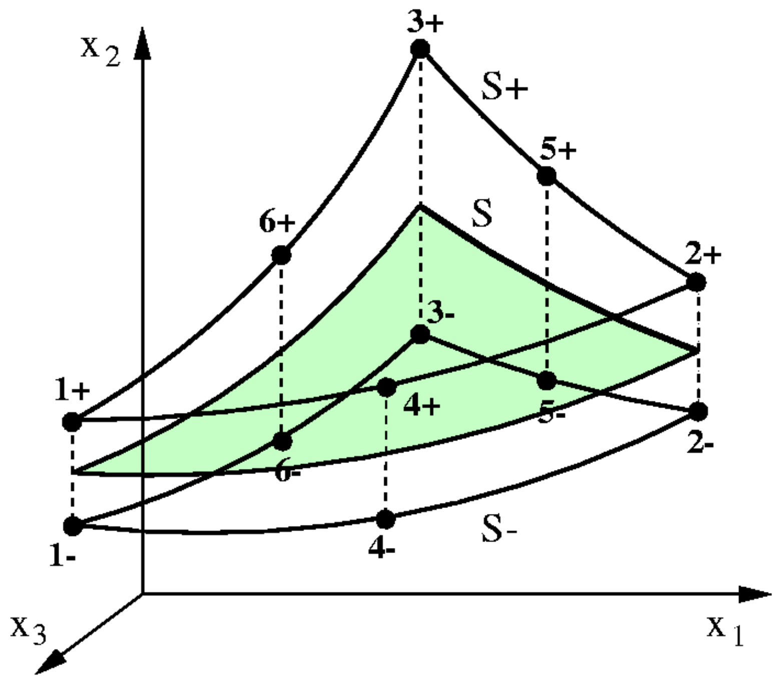

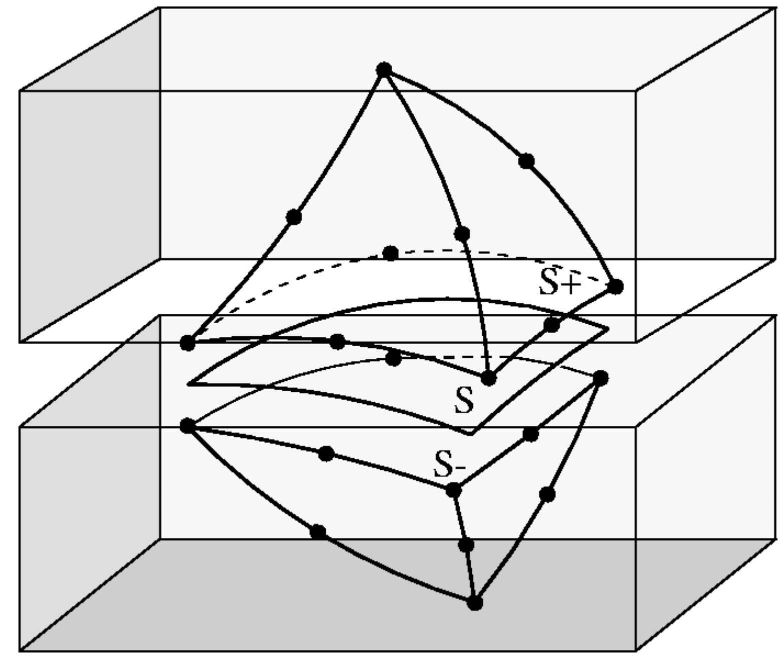

12-node quadratic cohesive elements
(Ortiz and Pandolfi, 1999)

Michael
Ortiz

Cohesive elements - Convergence

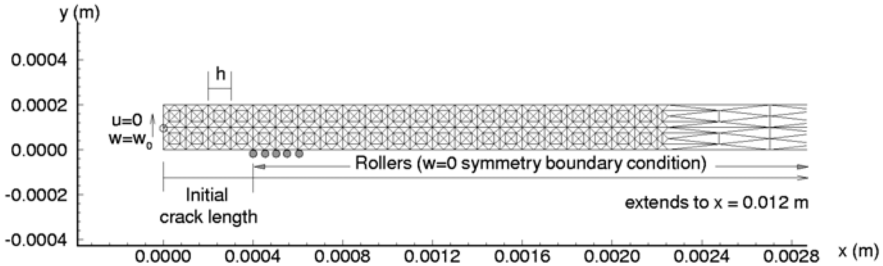

Double cantilever specimen

- Characteristic size:

$$l_c = \frac{\pi}{8} \frac{E}{1-\nu^2} \frac{G_c}{\sigma_c^2}$$

- Characteristic time:

$$t_c = \frac{l_c}{c_R}$$

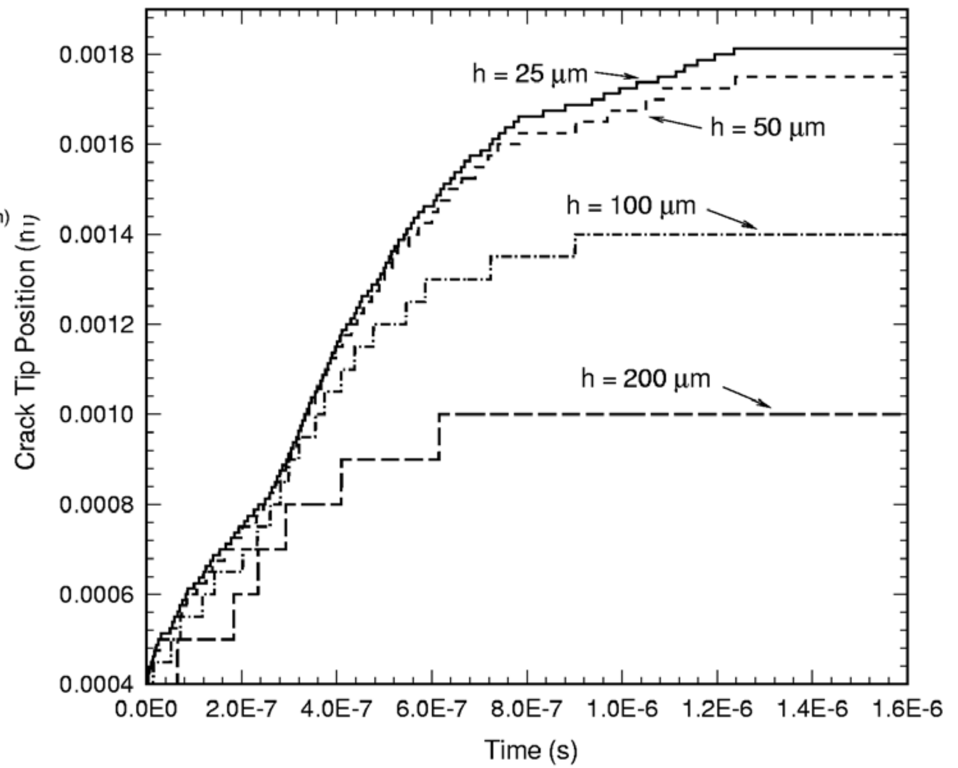

Crack-tip trajectory
as a function of element size
(Camacho and Ortiz, 1996)

Michael
Ortiz

Cohesive elements - Convergence

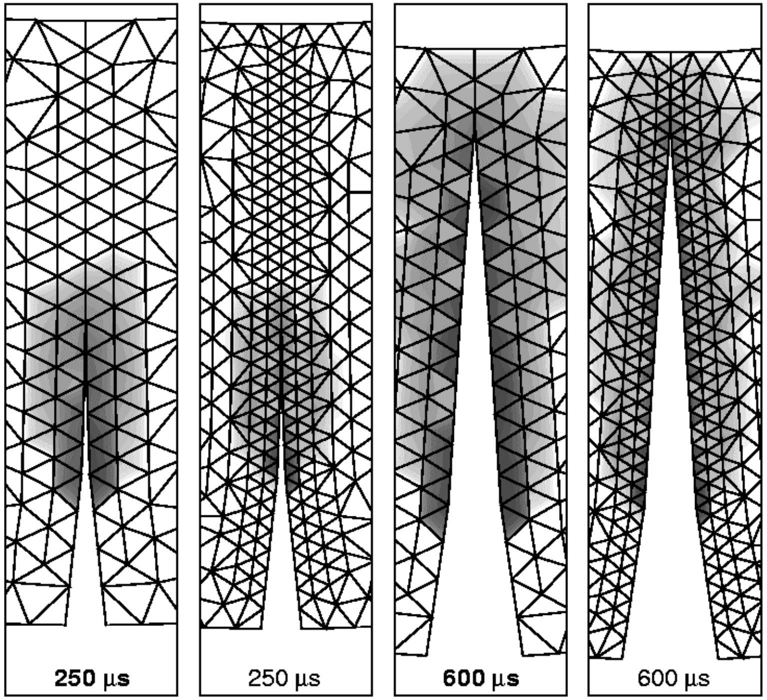

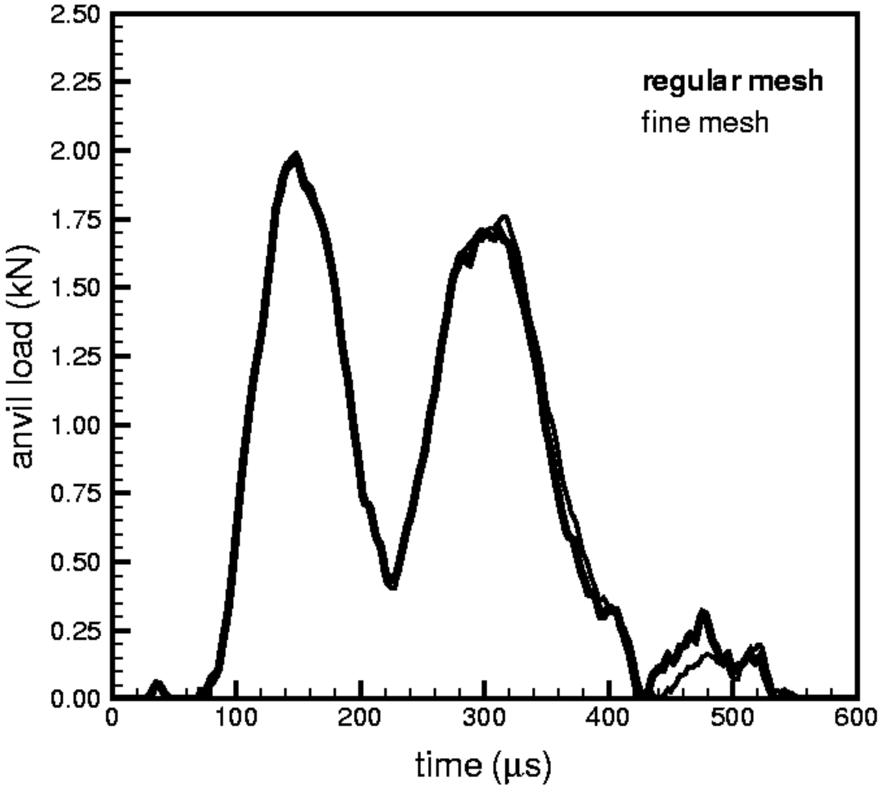

Dynamic three-point bend test - Prenotched specimen
Crack-tip trajectory and contours of damage
for coarse and fine meshes
(Ruiz, Pandolfi and Ortiz, 2000)

Michael
Ortiz

Cohesive elements - Convergence

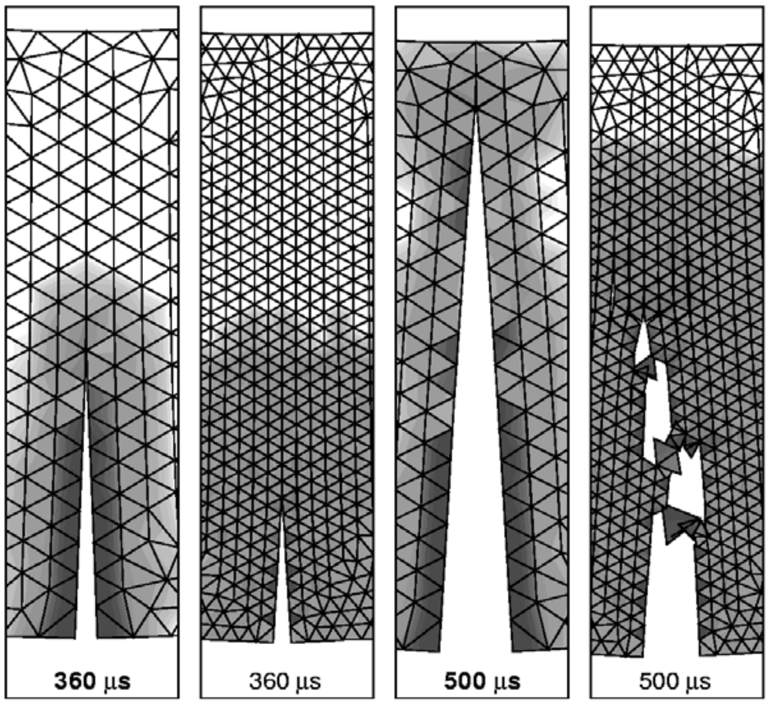

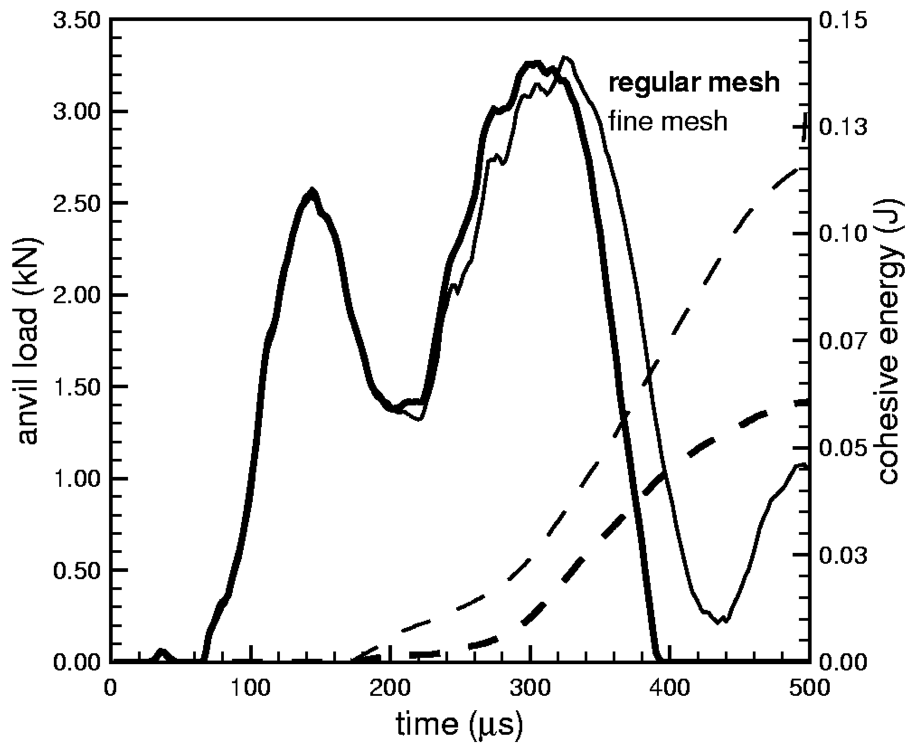

Dynamic three-point bend test - Nucleation
Crack-tip trajectory and contours of damage
for coarse and fine meshes
(Ruiz, Pandolfi and Ortiz, 2000)

Michael
Ortiz

Steel pellet vs. alumina plate

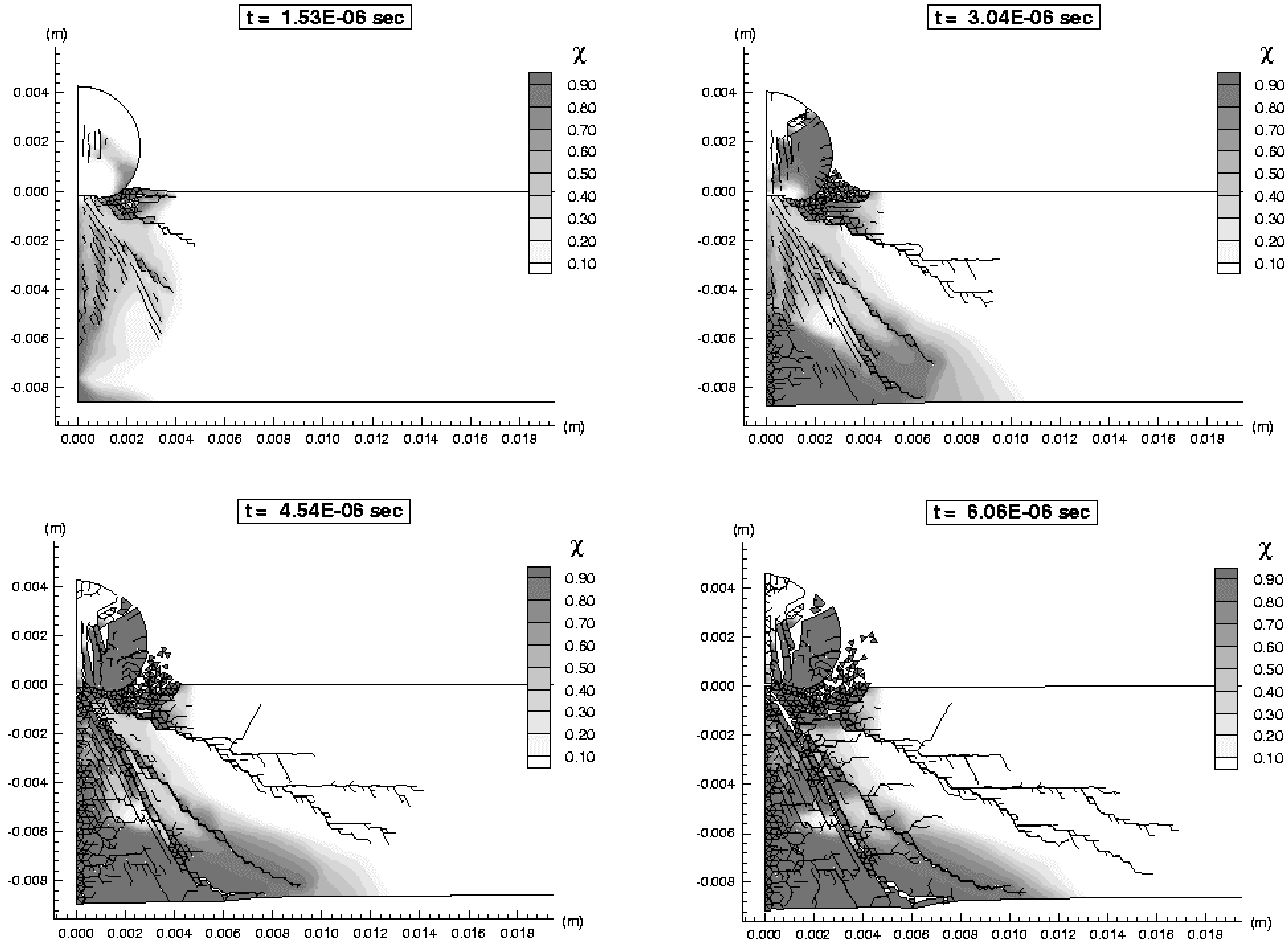

(Camacho and Ortiz, 1996; Field, 1988)

Michael Ortiz

WHA long rod vs. alumina plate

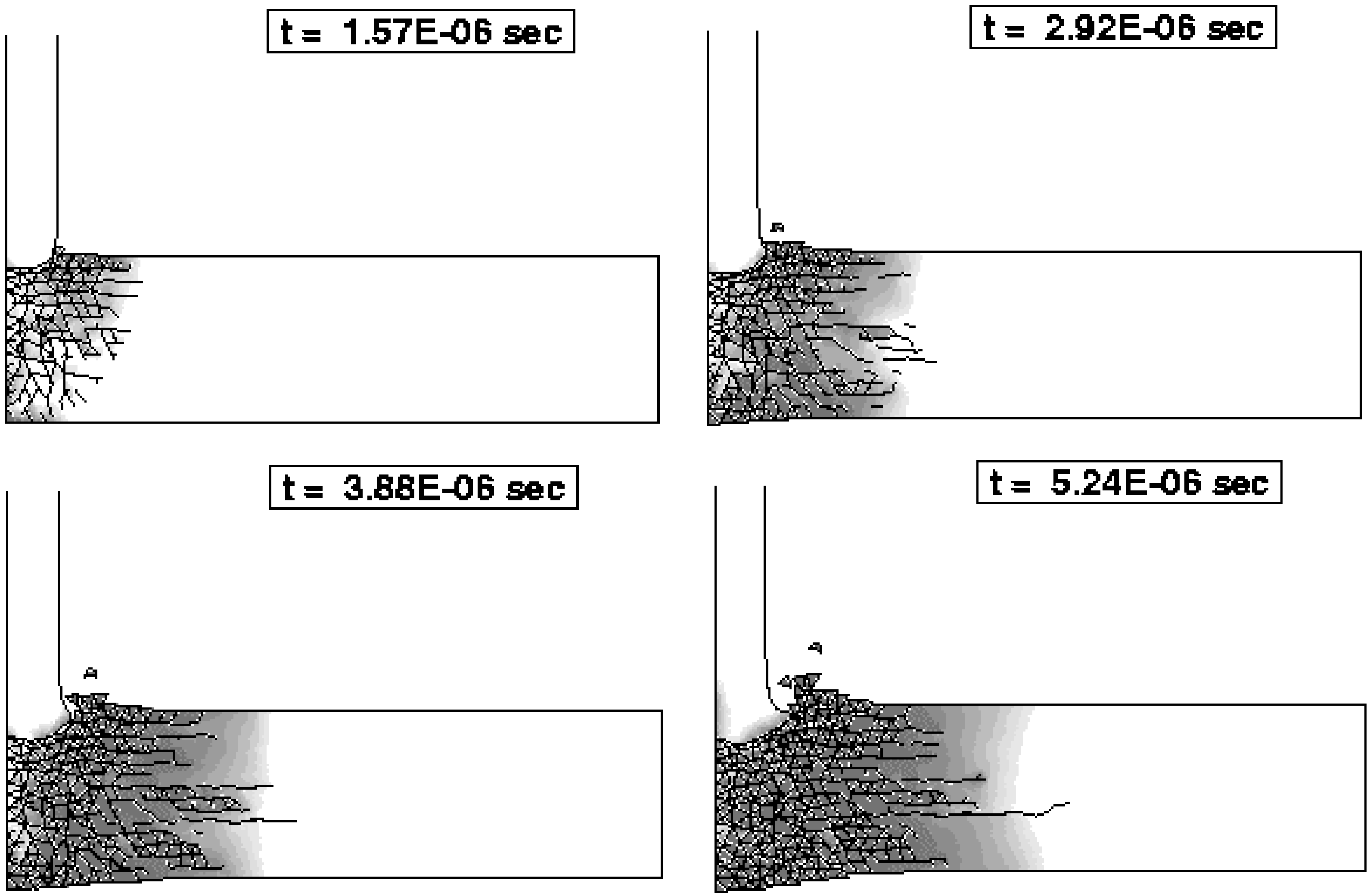

(Camacho and Ortiz, 1996; Woodward et al., 1994)

Michael Ortiz

WHA long rod vs. alumina plate

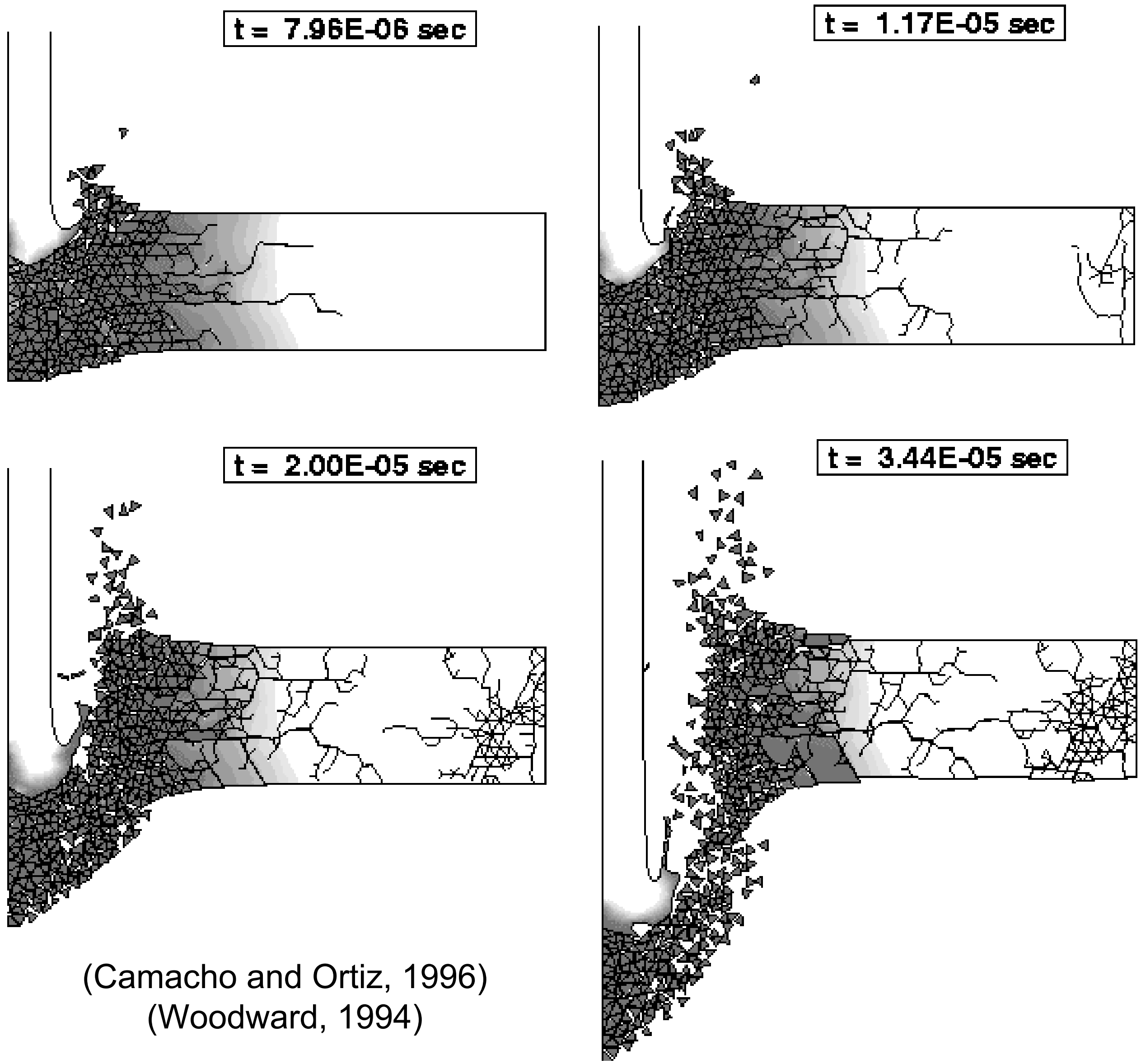

(Camacho and Ortiz, 1996)
(Woodward, 1994)

Michael Ortiz

WHA long rod vs. confined ceramic plate

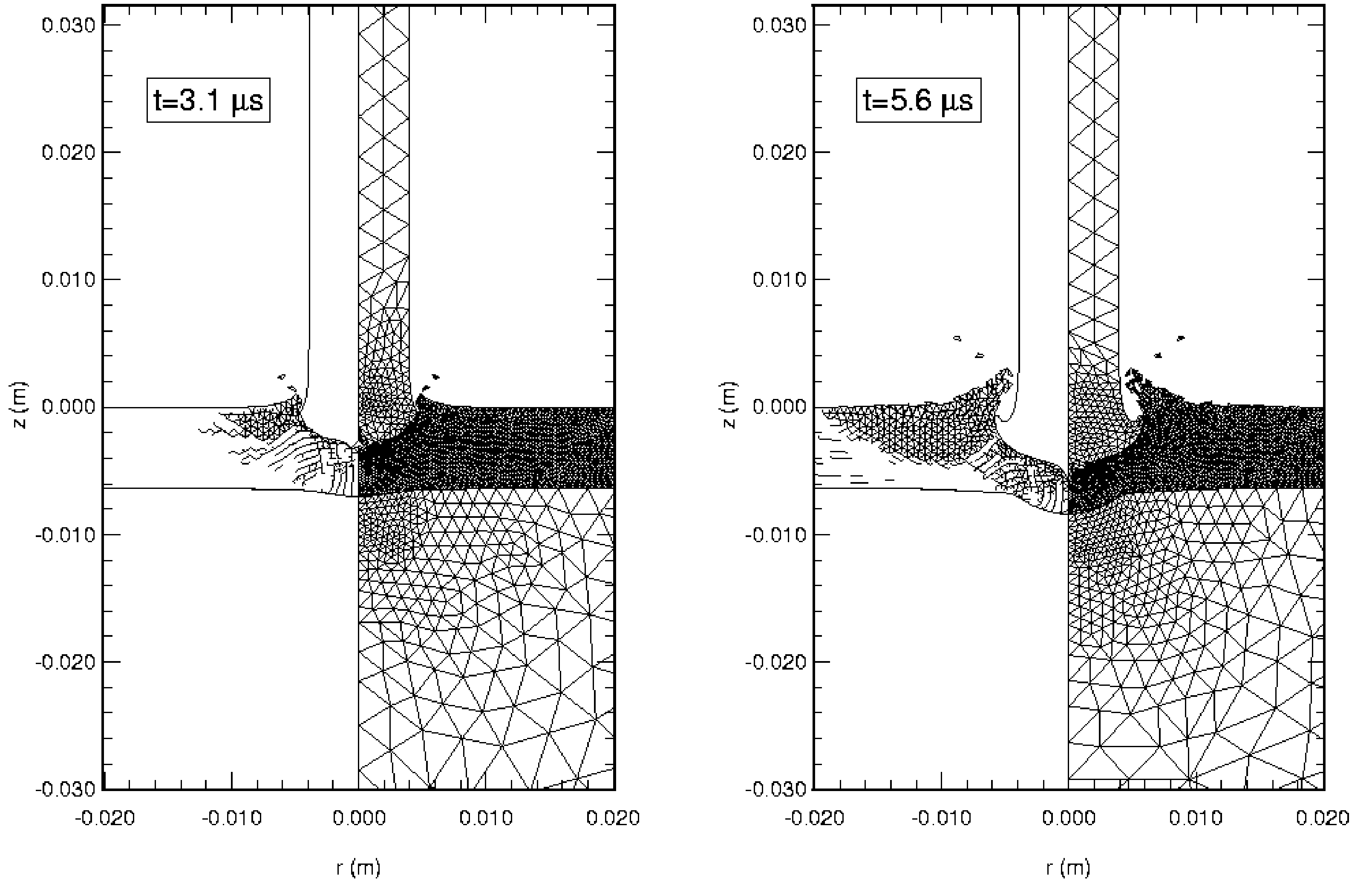

(Camacho and Ortiz, 1996; Grace and Rupert, 1994)

Michael Ortiz

WHA long rod vs. confined ceramic plate

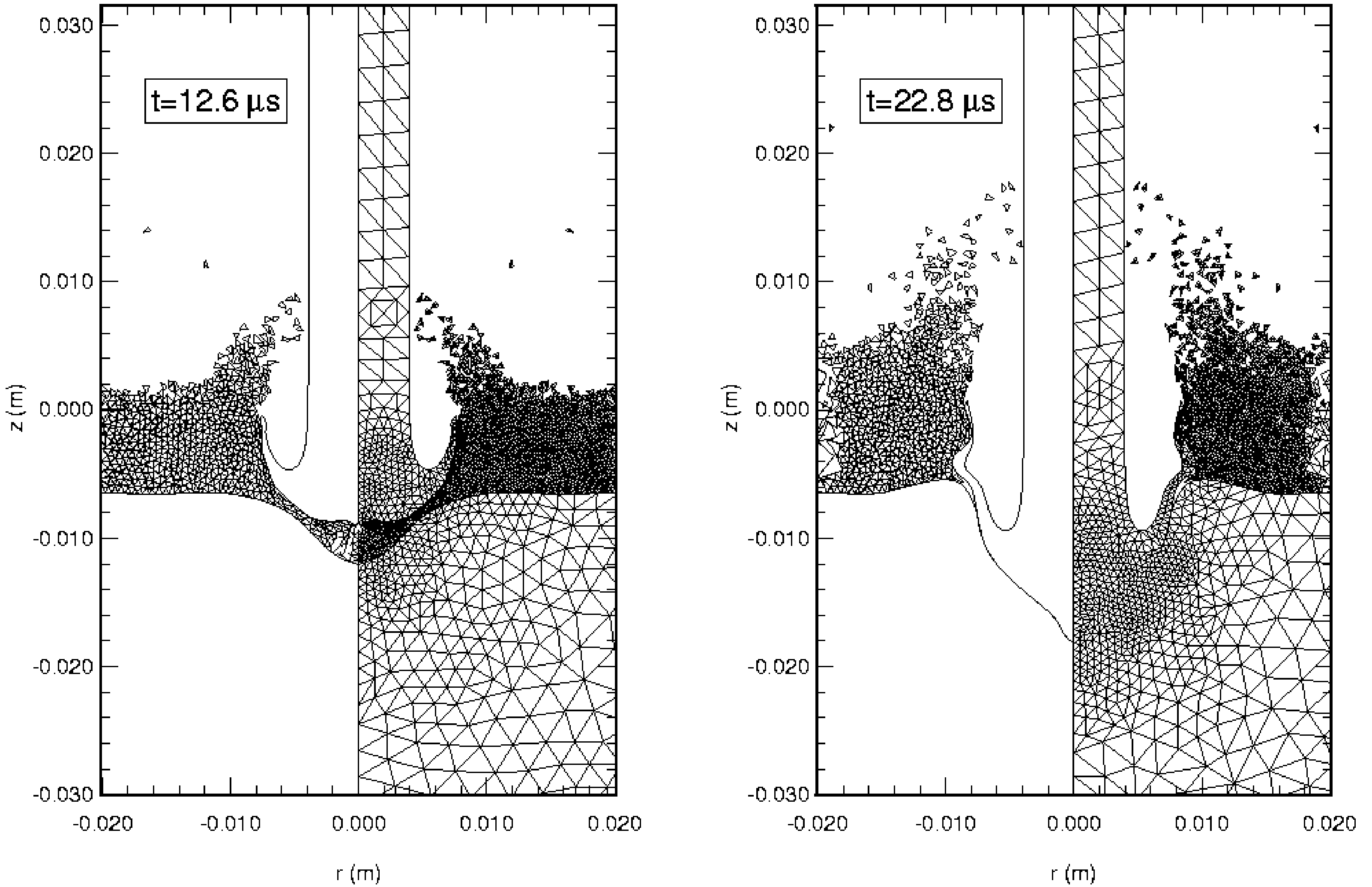

(Camacho and Ortiz, 1996; Grace and Rupert, 1994)

Michael Ortiz

Failure waves in glass rods

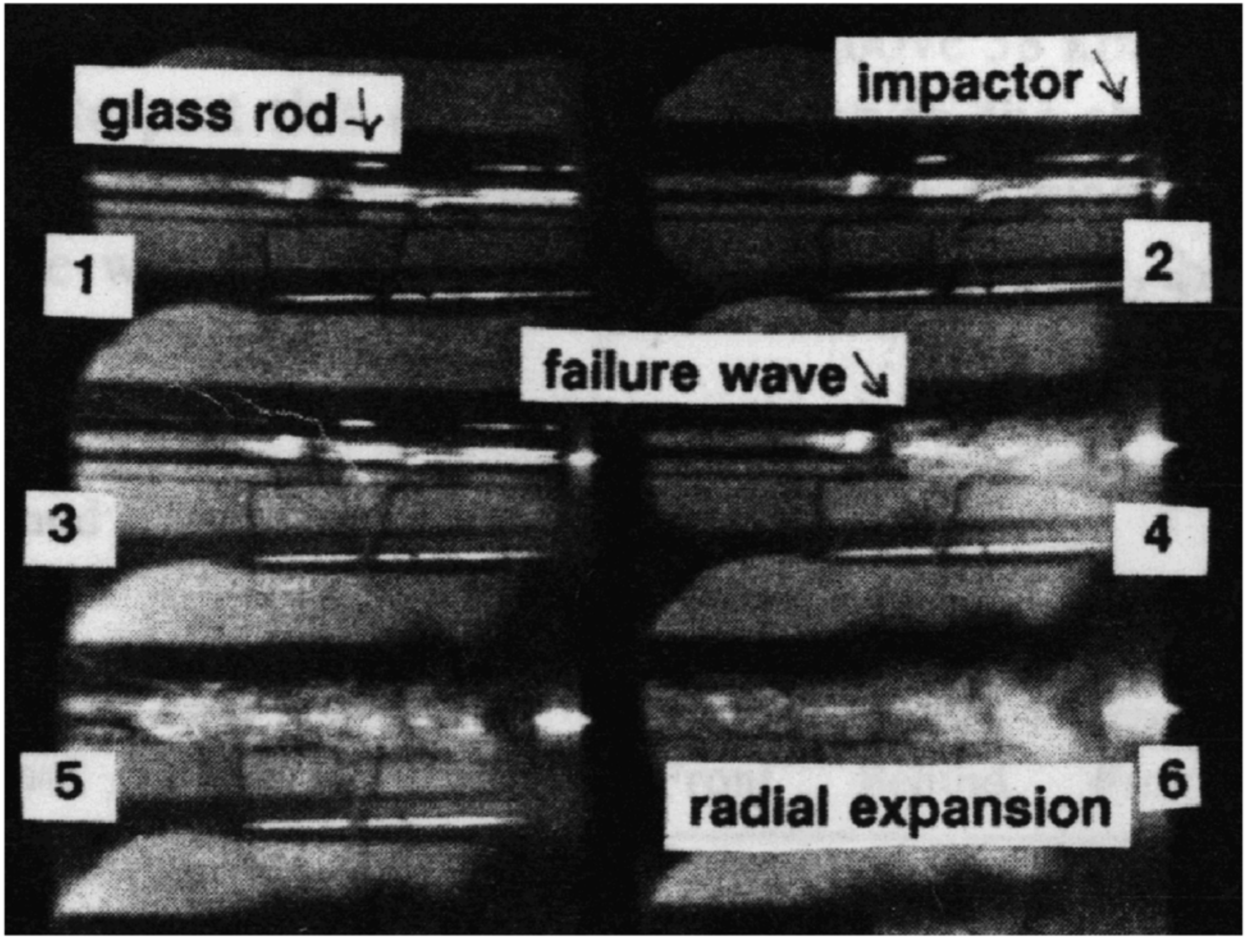

(Brar, Bless and Rosenberg, 1991)
(Repetto, Radovitzky and Ortiz, 2000)

Michael Ortiz

Failure waves in glass rods

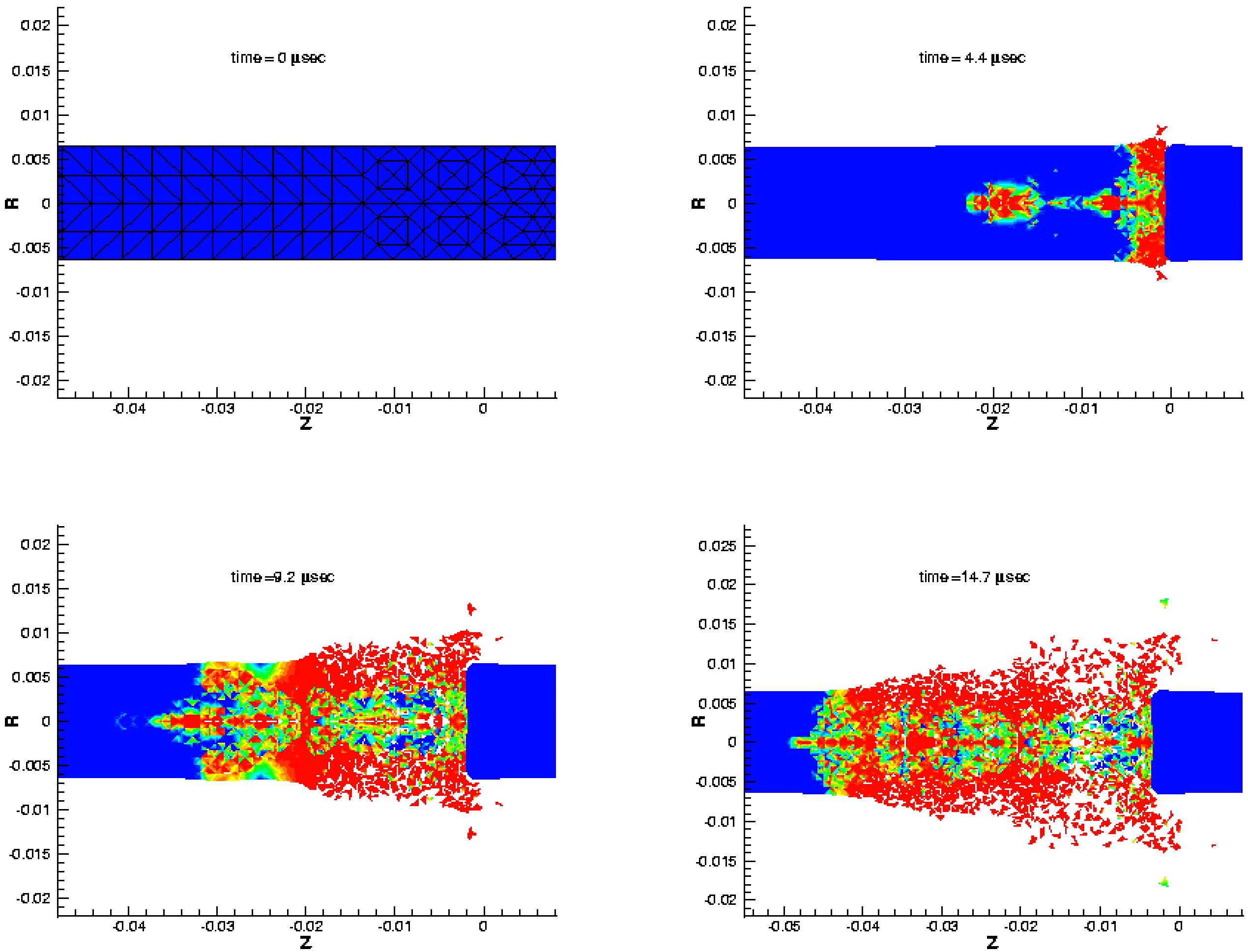

(Repetto, Radovitzky and Ortiz, 2000)
(Brar, Bless and Rosenberg, 1991)

(movie)

Michael Ortiz

Mixed-mode Charpy test

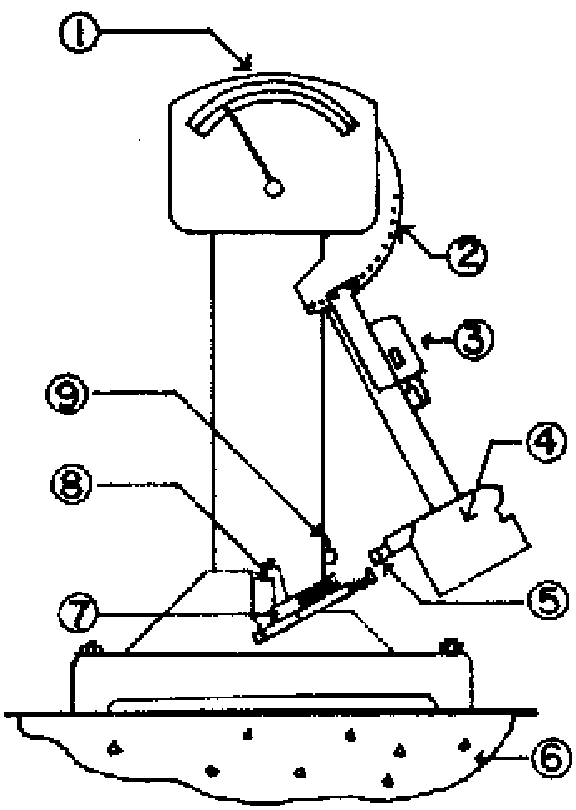

(John and Shah, 1990)

(Guo et al., 1995)

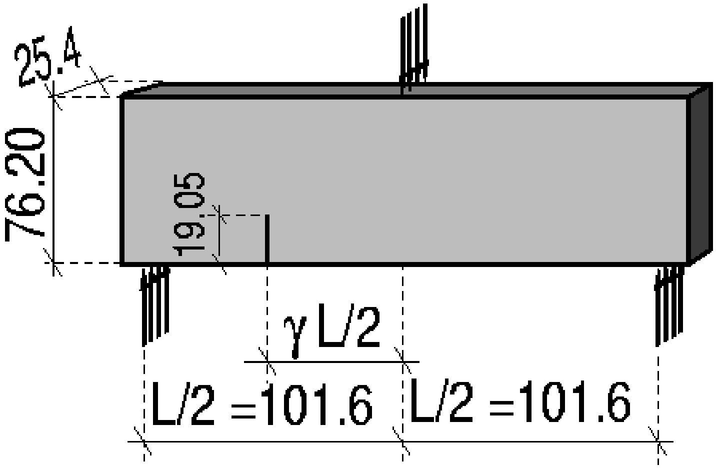

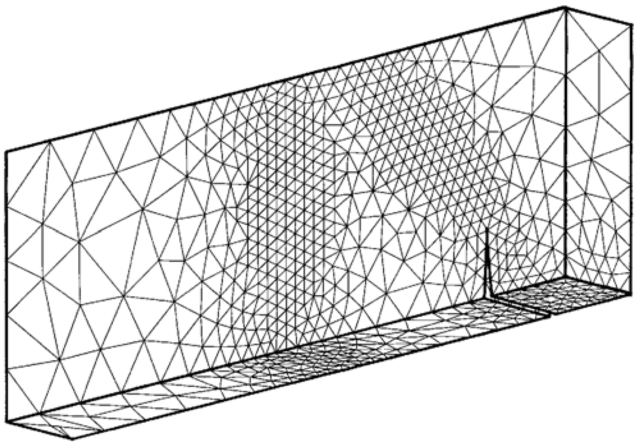

(Ruiz, Pandolfi and Ortiz, 2000)

Michael
Ortiz

Mixed-mode Charpy test

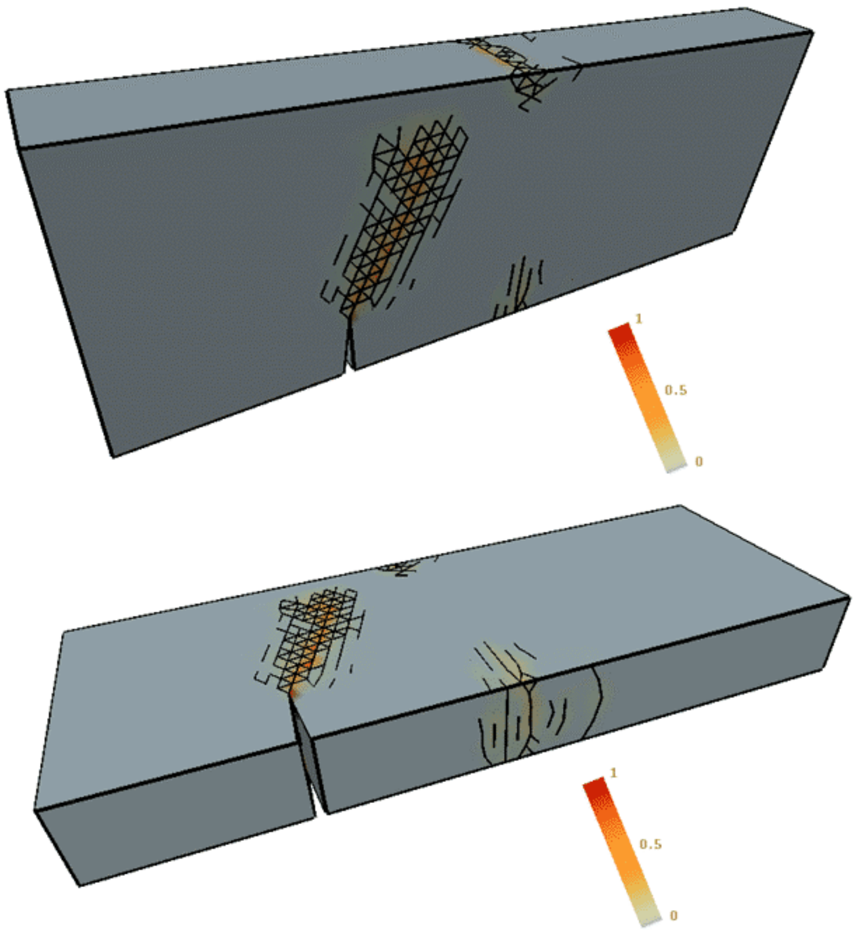

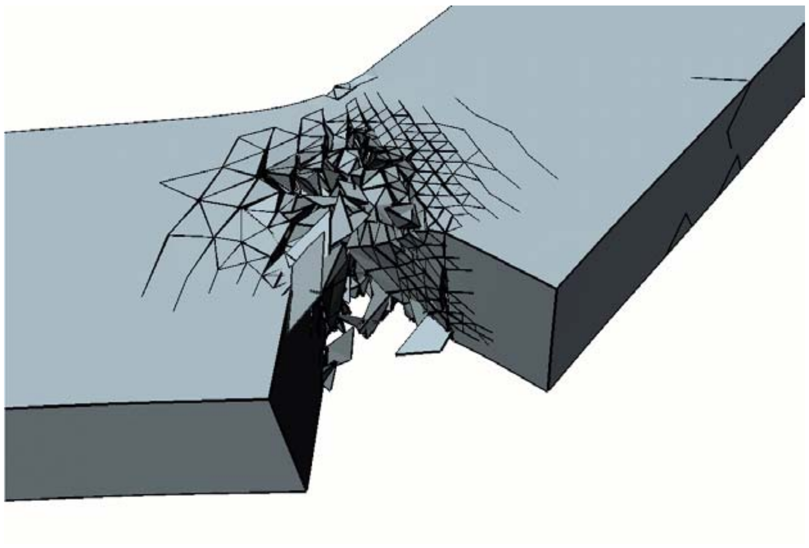

(Ruiz, Pandolfi and Ortiz, 2000)

Mixed-mode Charpy test

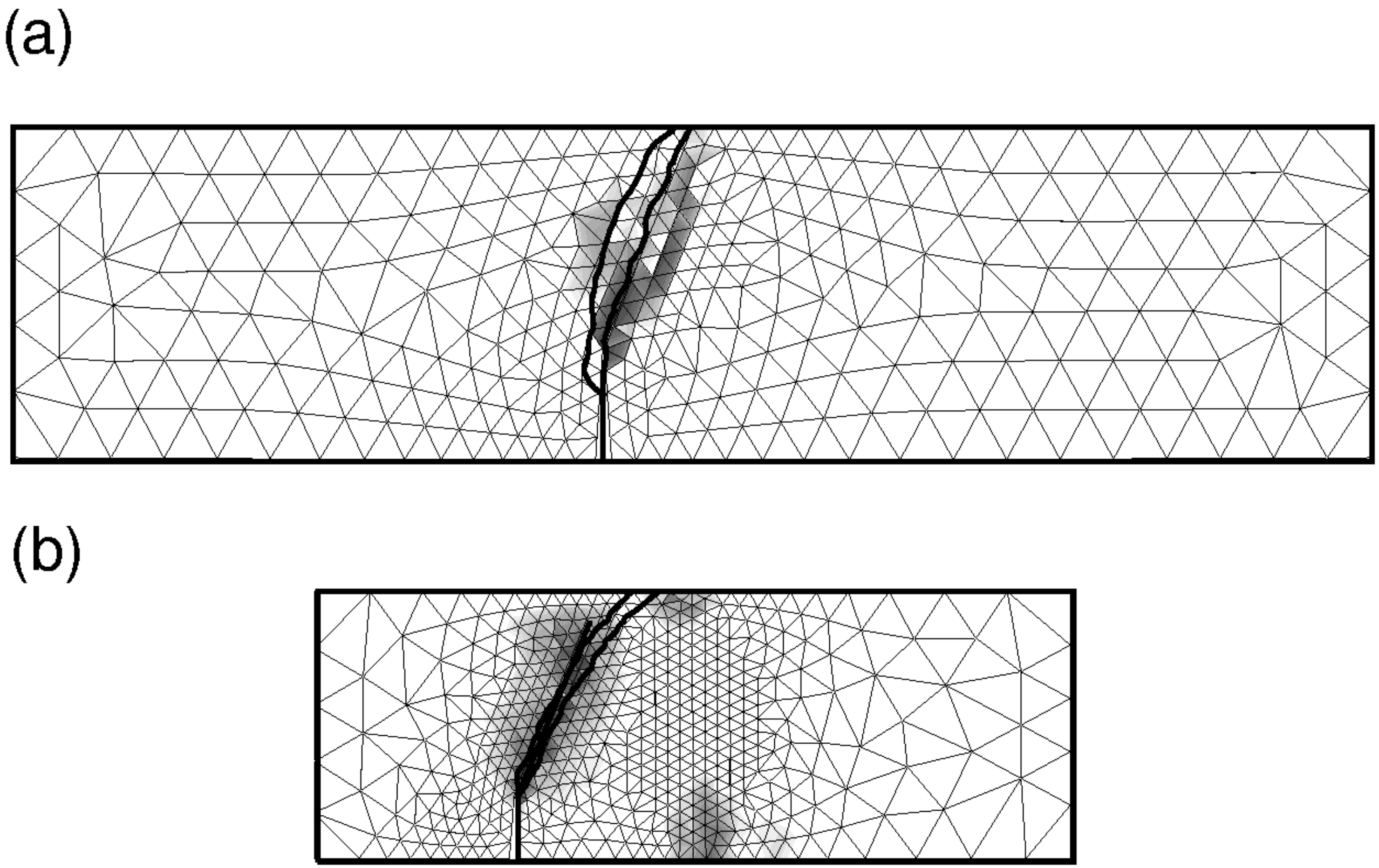

Computed and experimental crack paths.
a) Guo et al., 1995; b) John and Sha, 1990.
(Ruiz, Pandolfi and Ortiz, 2000)

Mixed-mode Charpy test

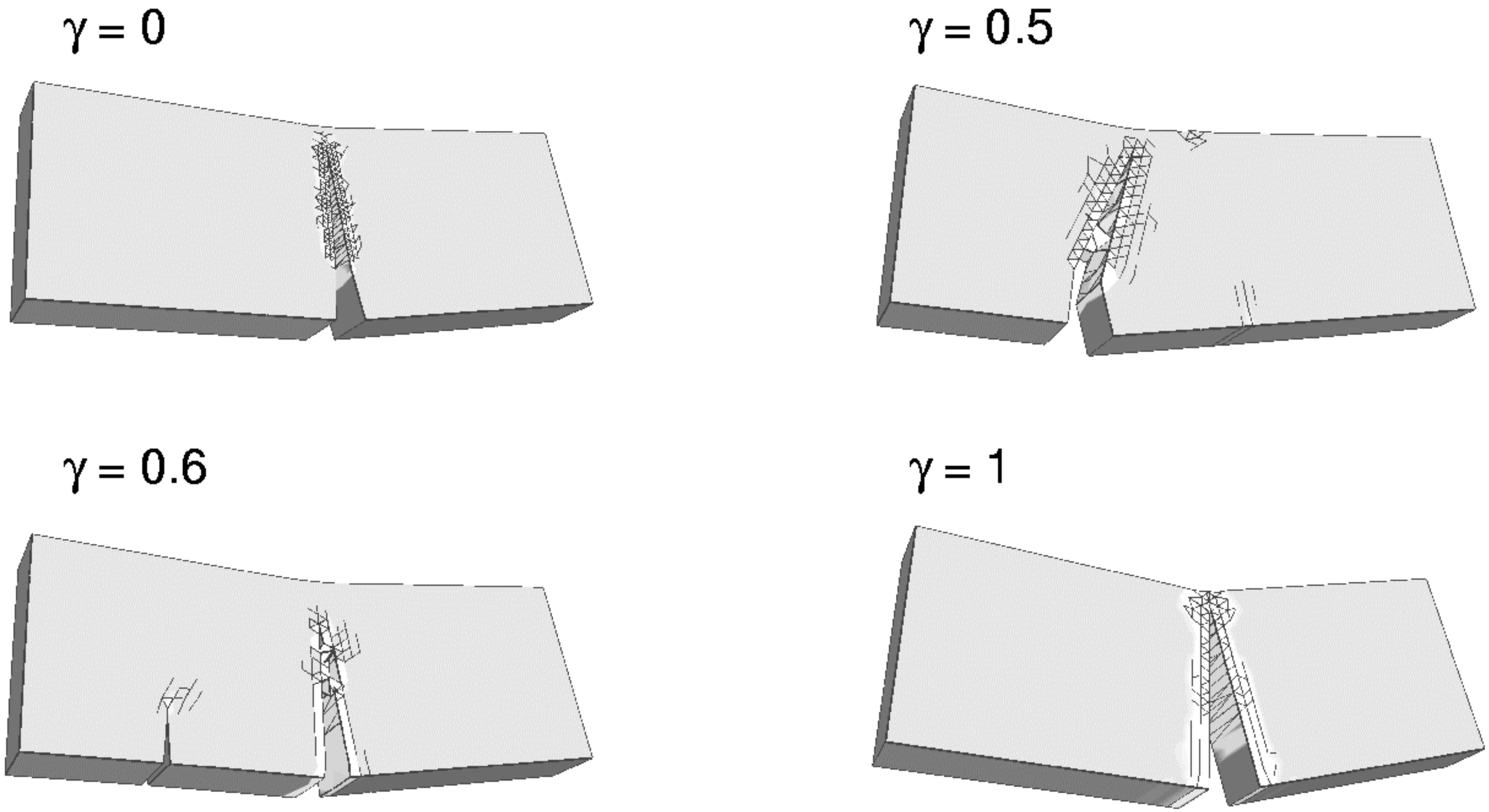

Influence of crack offset on crack pattern
(Ruiz, Pandolfi and Ortiz, 2000)

Michael
Ortiz

Drop-weight test - C300 steel

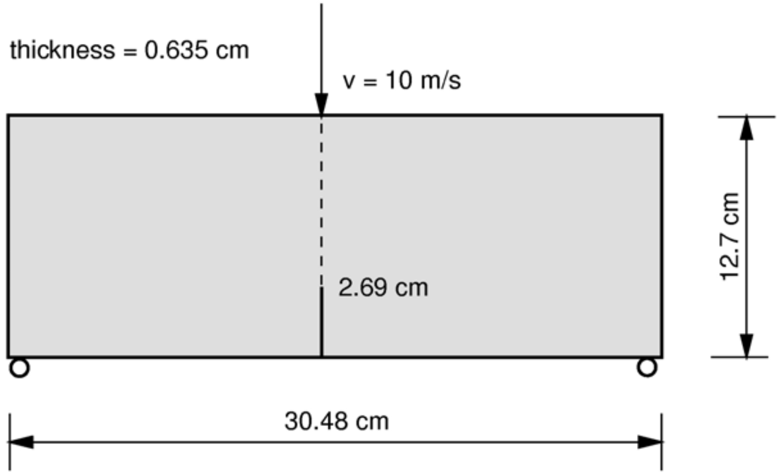

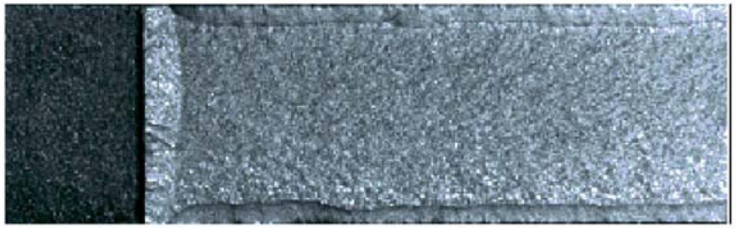

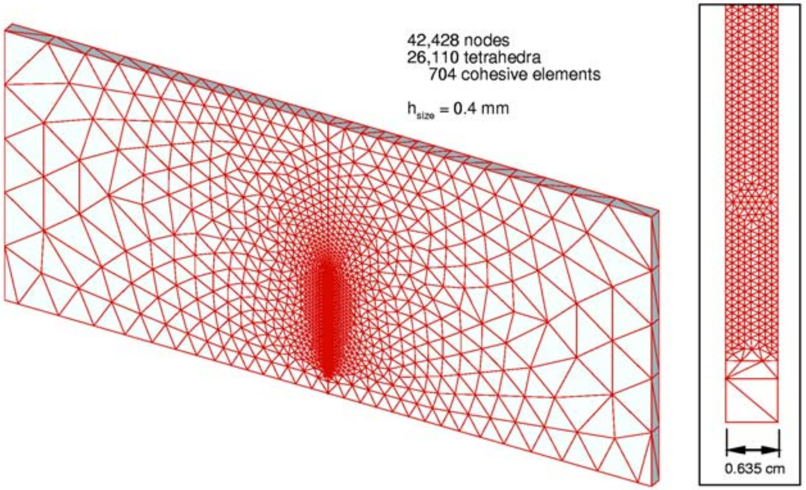

(Pandolfi, Guduru, Ortiz and Rosakis, 2000)

Michael
Ortiz

Drop-weight test - C300 steel

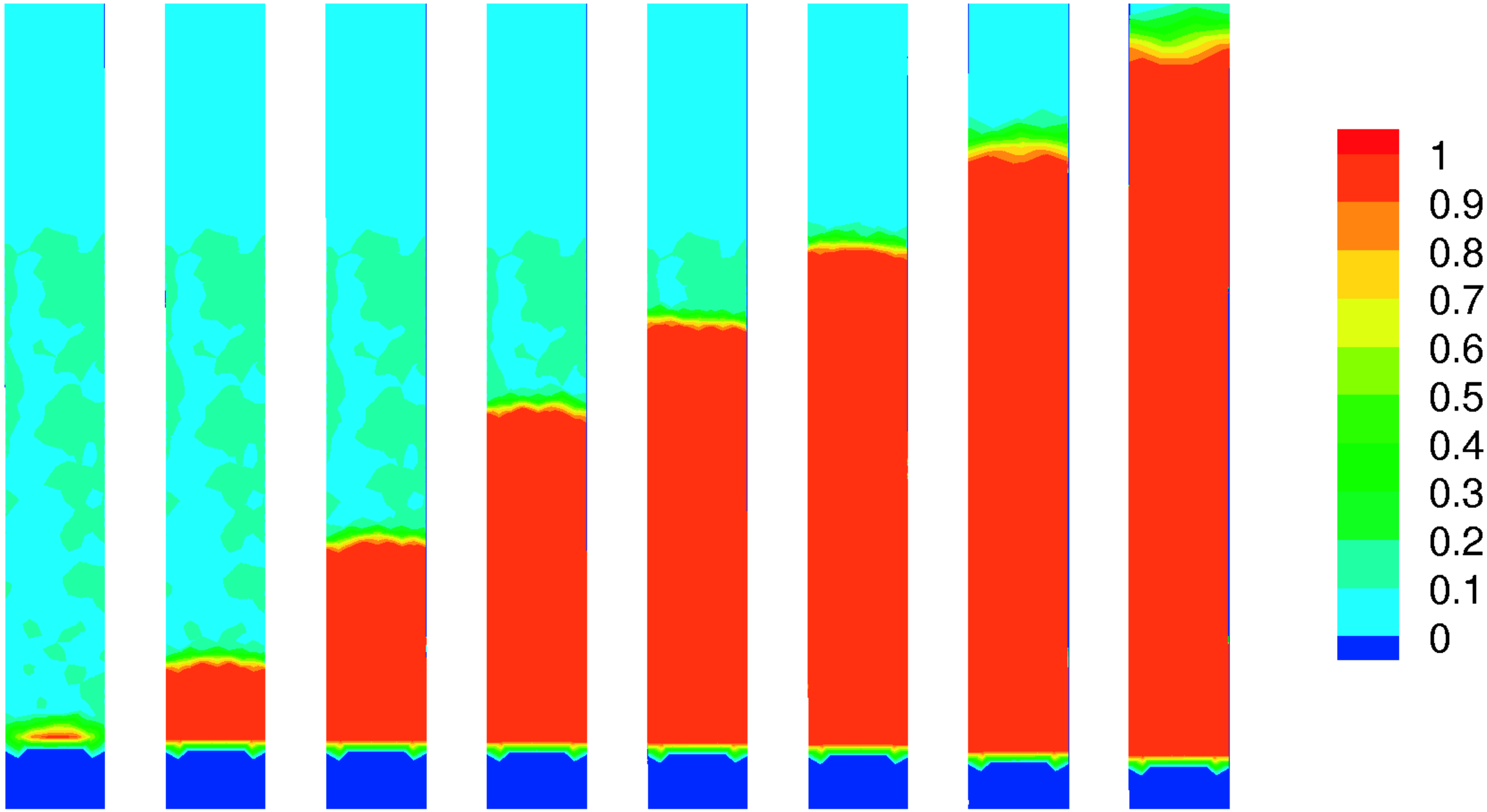

Crack geometry as a function of time
(Pandolfi, Guduru, Ortiz and Rosakis, 2000)

Michael
Ortiz

Drop-weight test - C300 steel

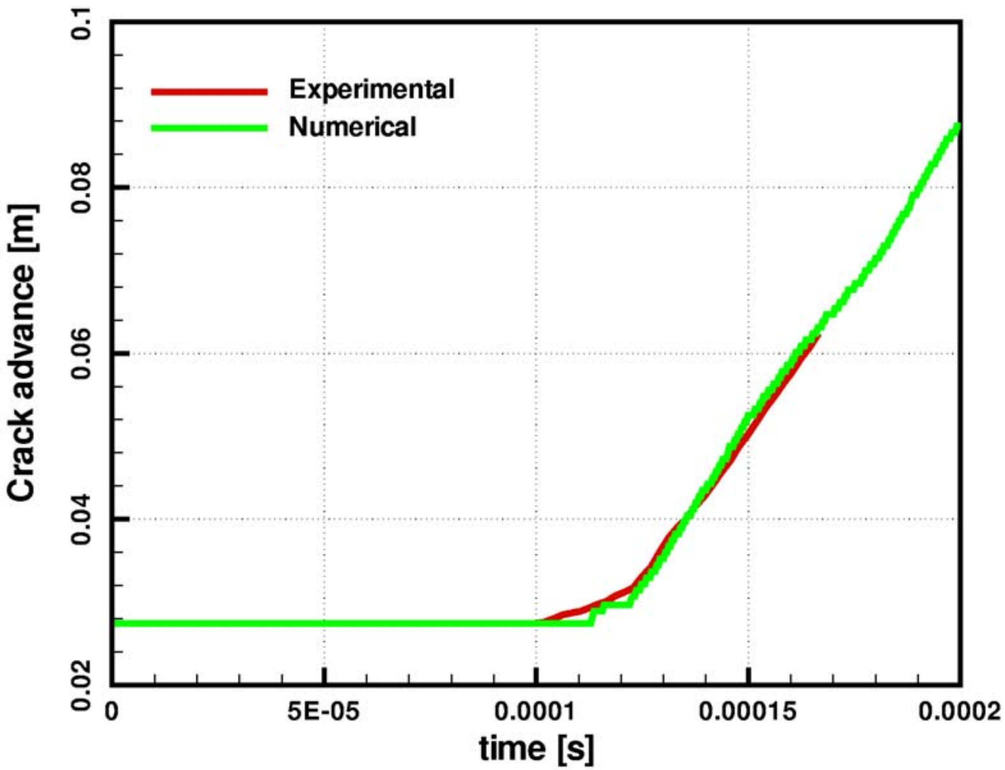

Computed vs. experimential crack-tip trajectory.

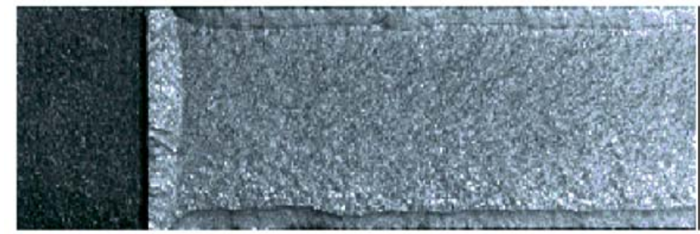

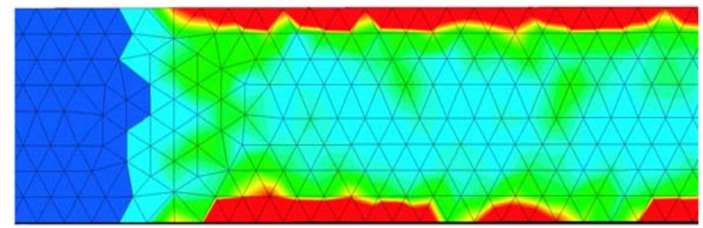

Plastic zone and shear-lip formation (Impact velocity = 10 m/s)

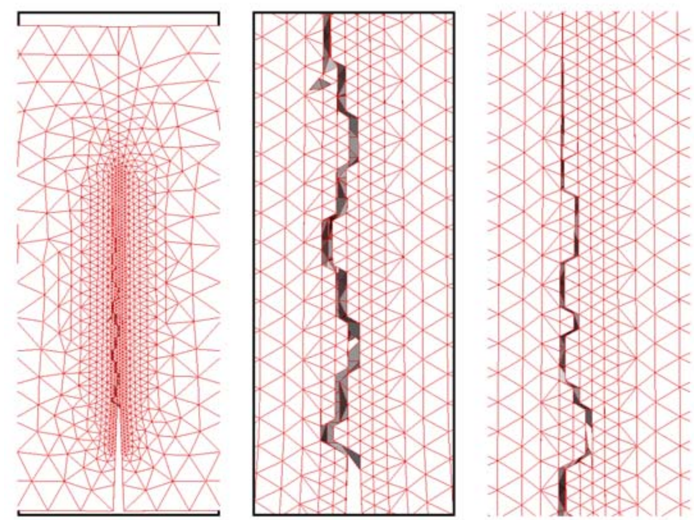

(Pandolfi, Guduru, Ortiz and Rosakis, 2000)

Michael Ortiz

Ring expansion test - Aluminum

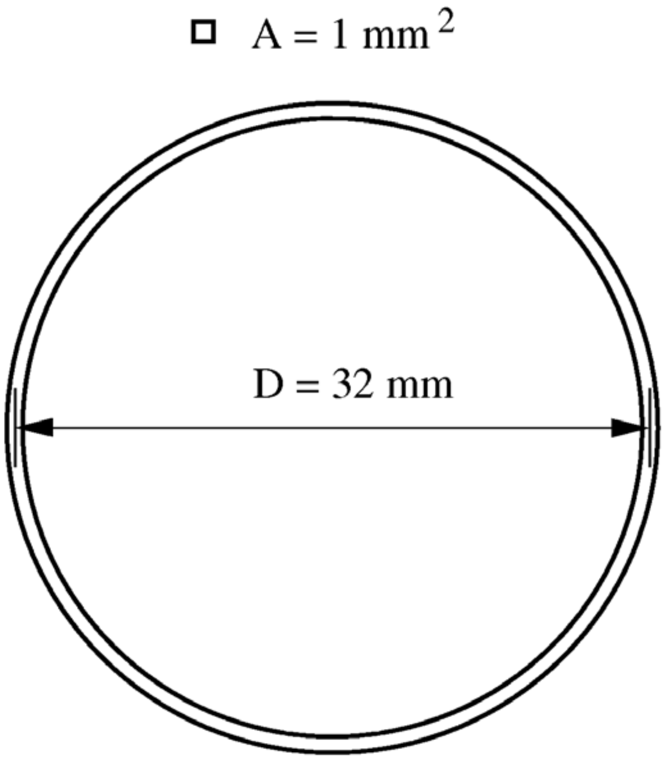

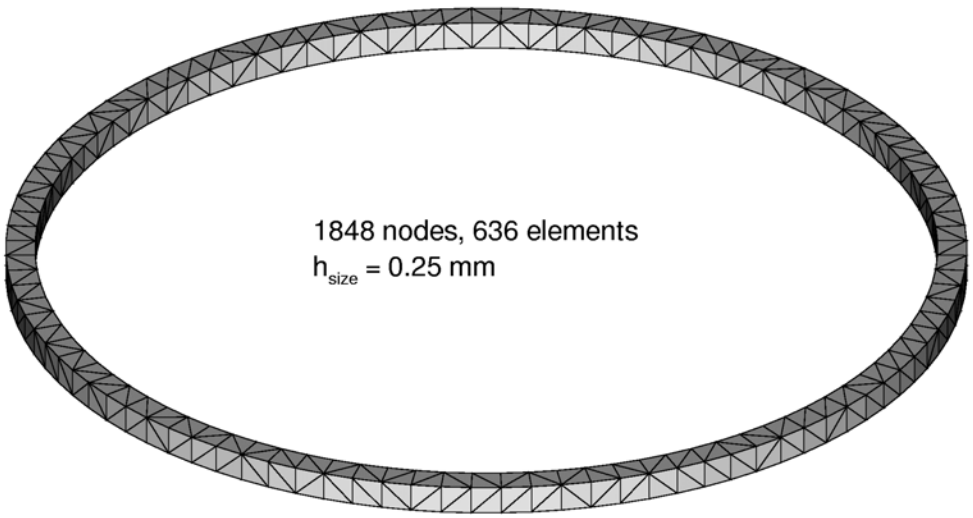

(Grady and Benson, 1983)
(Pandolfi, Krysl and Ortiz, 1999)

Michael Ortiz

Ring expansion test - Aluminum

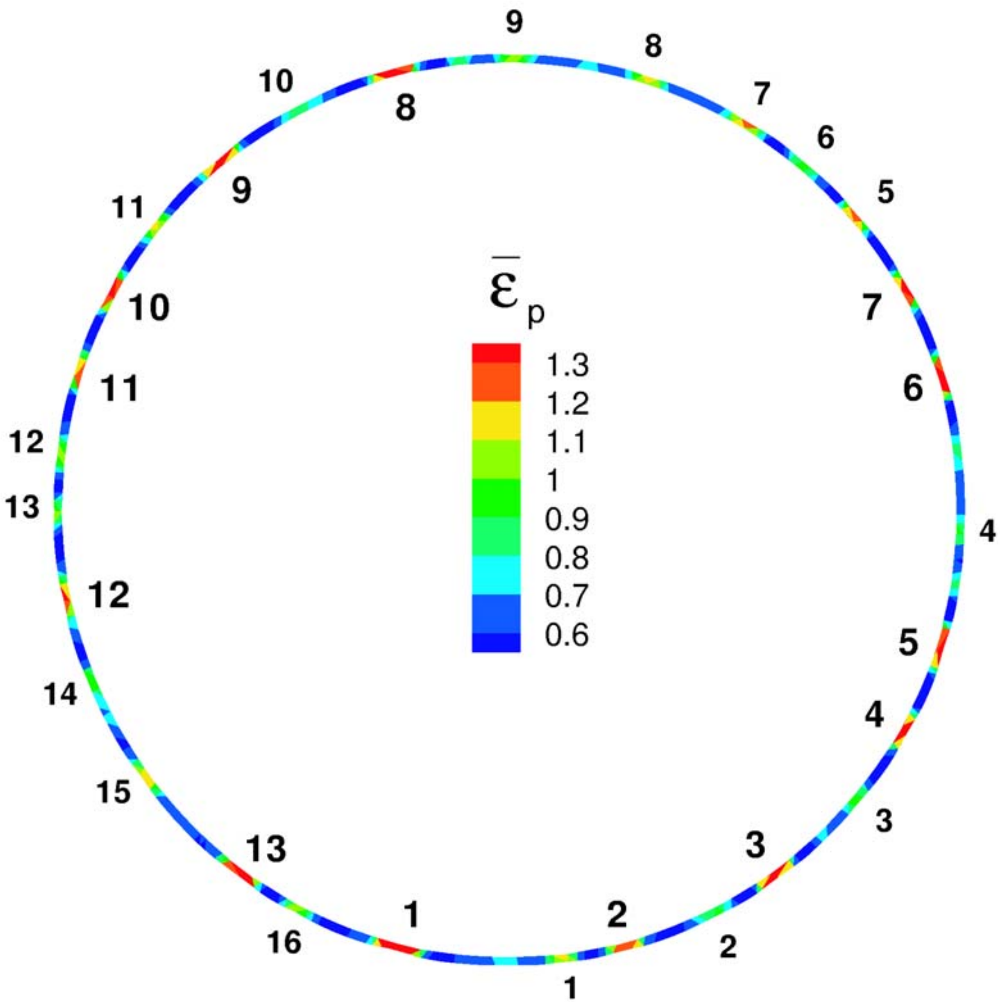

Active and inactive necks

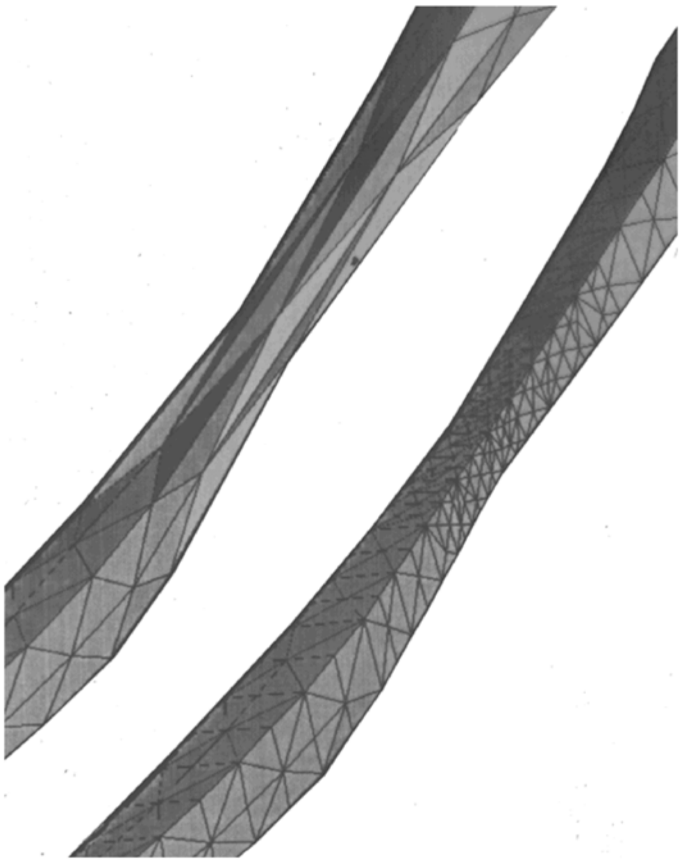

Detail of mesh refinement at necks

(Pandolfi, Krysl and Ortiz, 1999)

Michael Ortiz

Ring expansion test - Aluminum

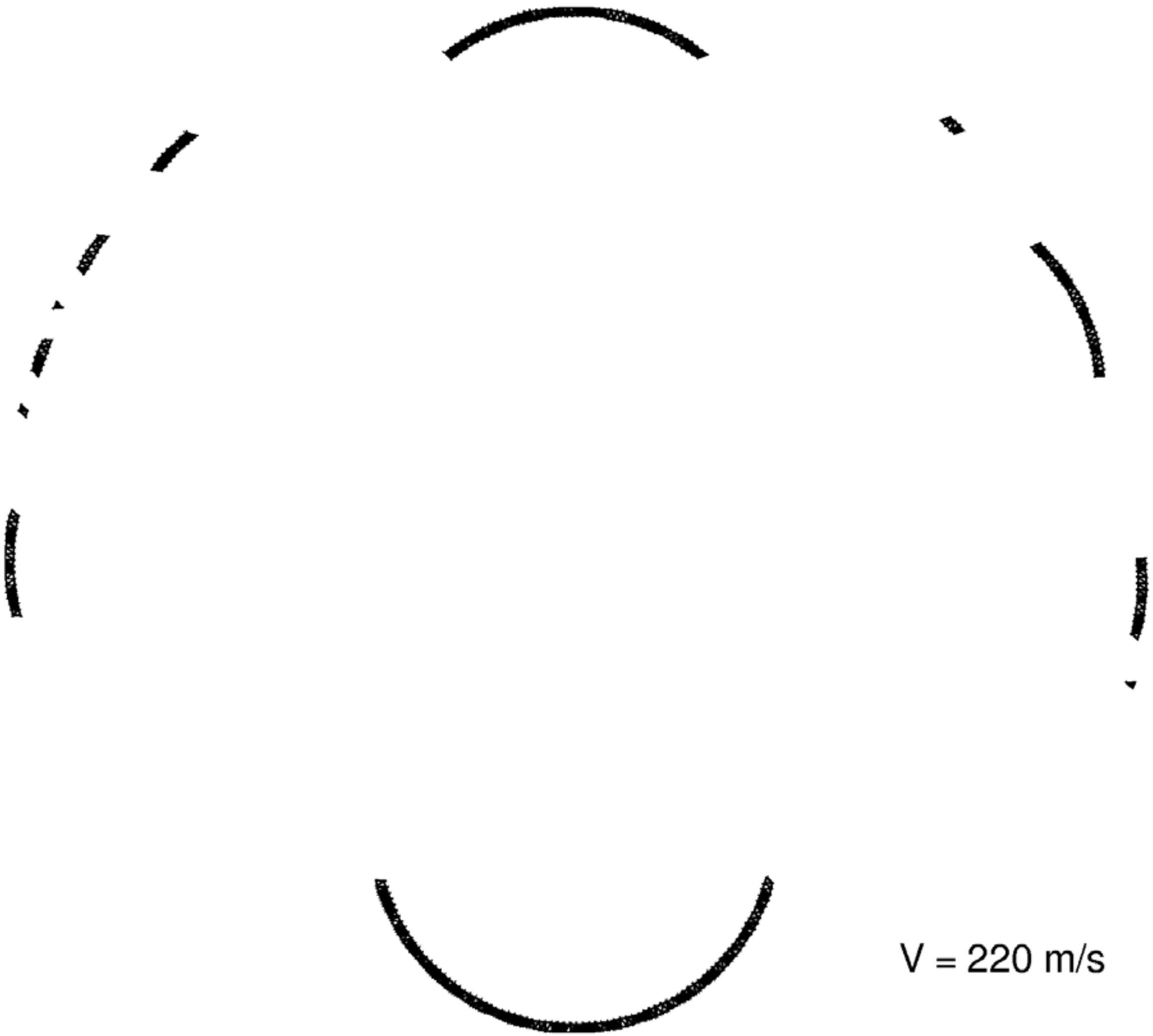

(Pandolfi, Krysl and Ortiz, 1999)

Michael Ortiz

Ring expansion test - Aluminum

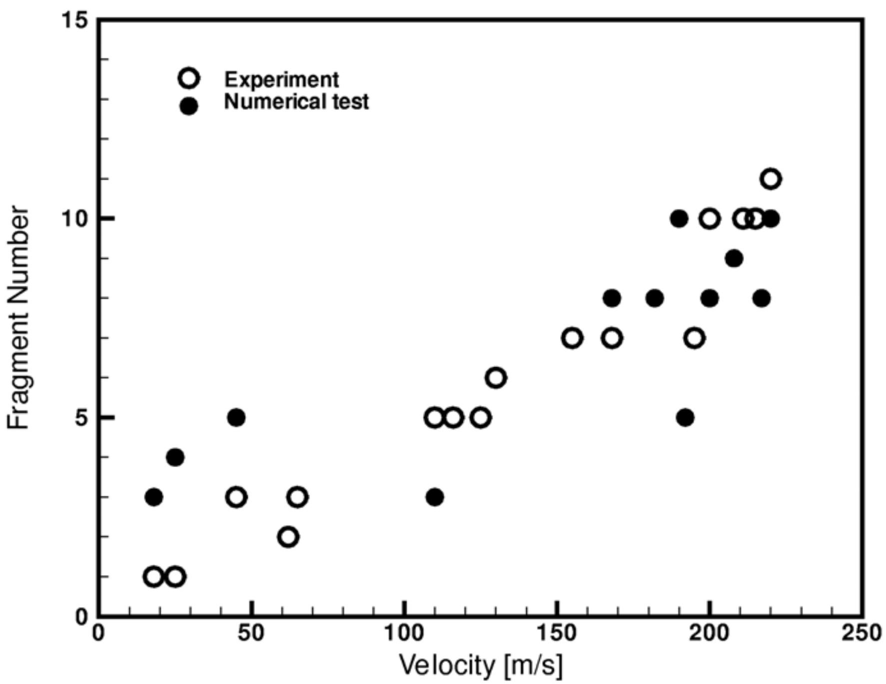

Number of fragments vs expansion velocity

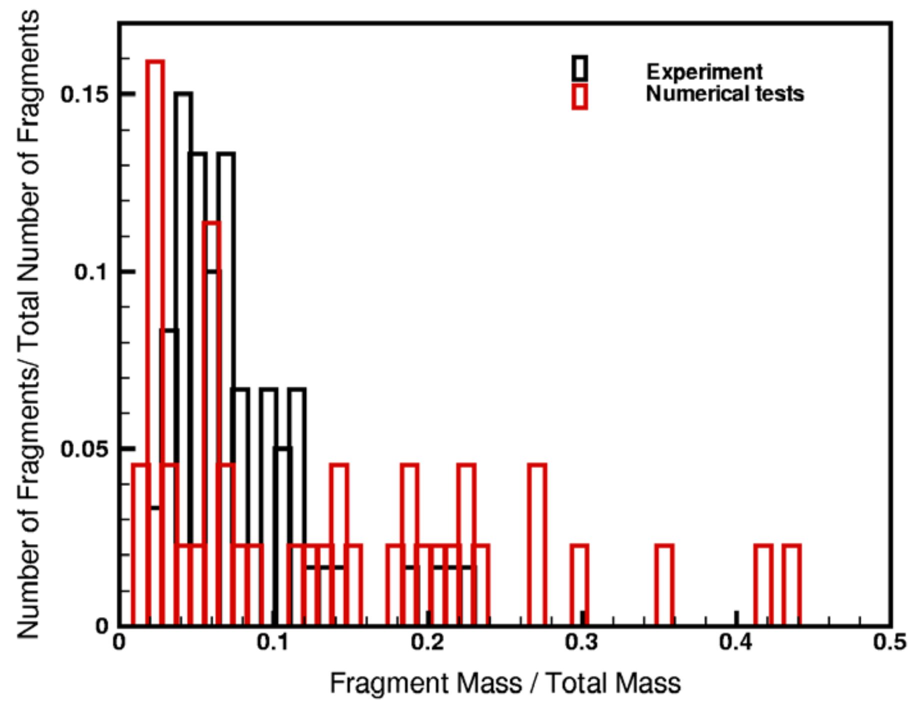

Fragment mass frequency distribution

(Pandolfi, Krysl and Ortiz, 1999)

Michael Ortiz

Fatigue crack growth - Cohesive models

- Reversible unloading:

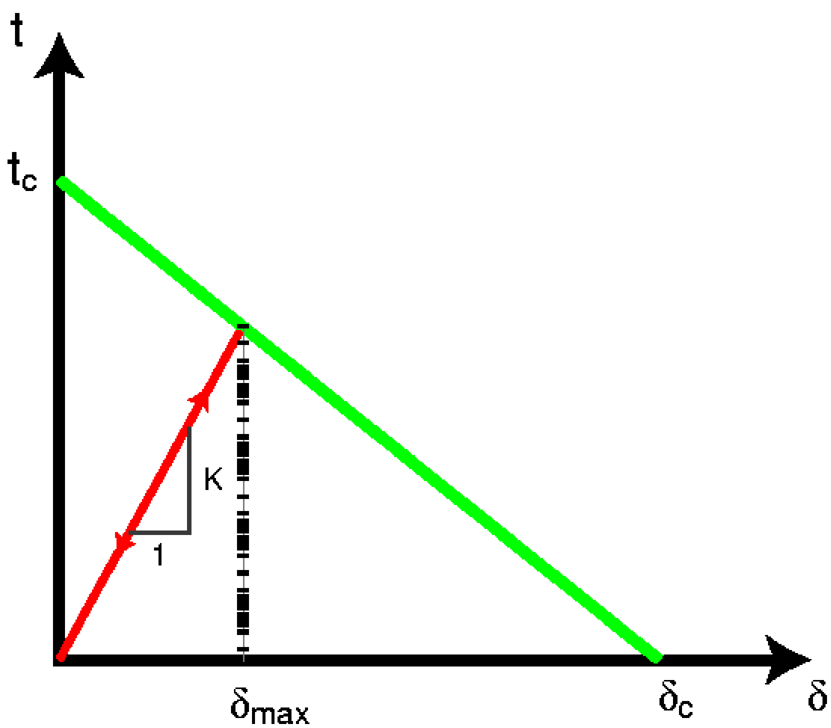

- Crack shakes down under cyclic loading.

- Loading-reloading hysteresis:

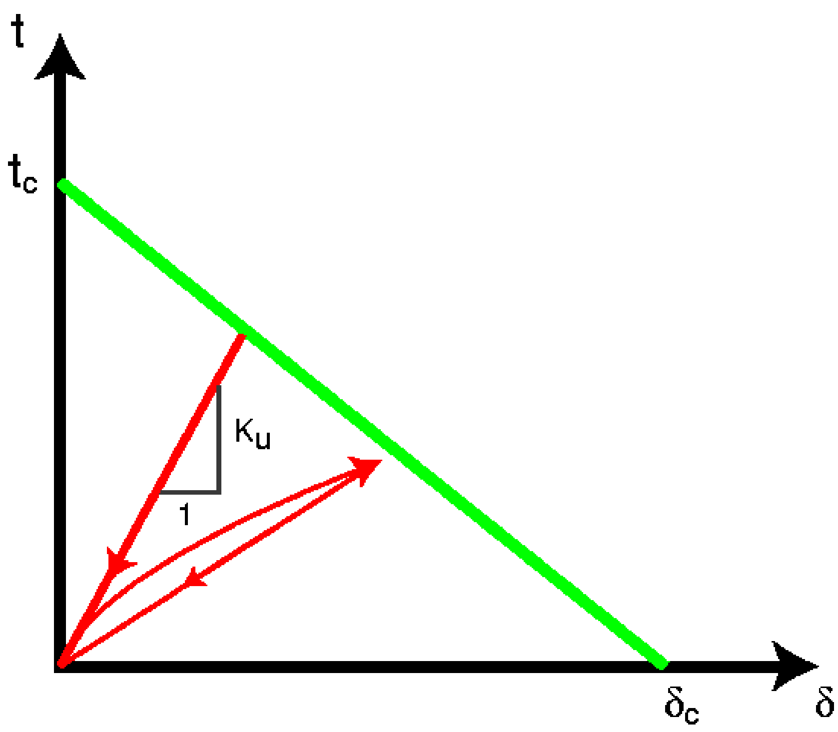

- Crack propagates under cyclic loading.

(Nguyen, Repetto and Ortiz, 2000)

Michael Ortiz

Case study: Al center-crack panel

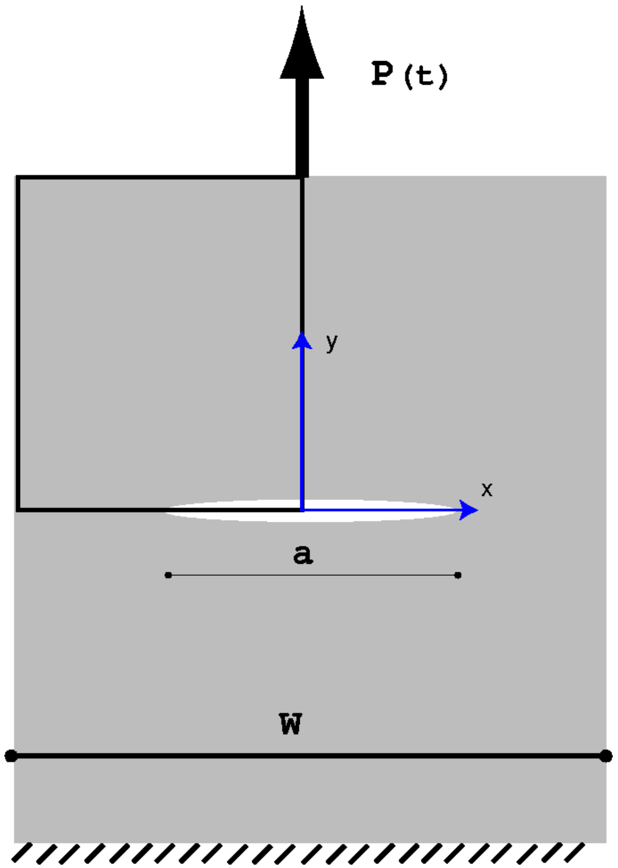

- Parameters (Al 2024-T351):

Young's modulus E	70 GPa
Poisson's ratio ν	0.3
Initial yield stress σ_0	325 MPa
Hardening exponent n	8
Reference plastic strain ε_0^p	0.0002
Specific cohesive energy G_c	13.8 KJ/m^2
Cohesive strength σ_c	800 MPa
Decay displacement δ_f	4 mm
Initial half-crack size a_0	10 mm
Applied stress amplitude σ_∞	85 MPa

Michael Ortiz

Fatigue crack growth - Long cracks

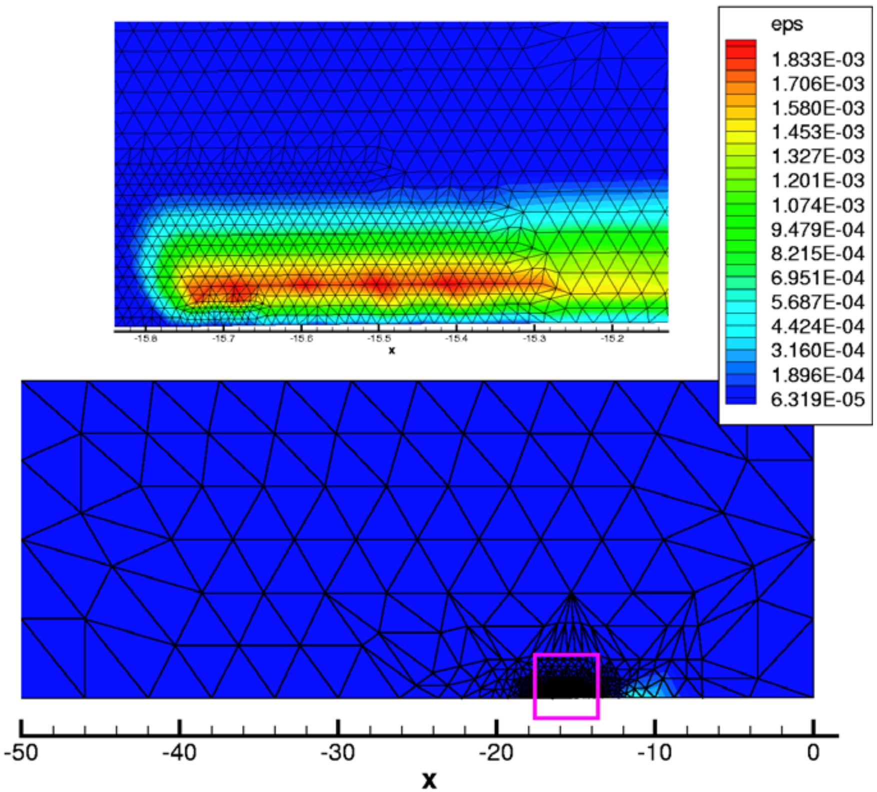

Contours of effective plastic strain.
Initial crack length: a = 15.72 mm

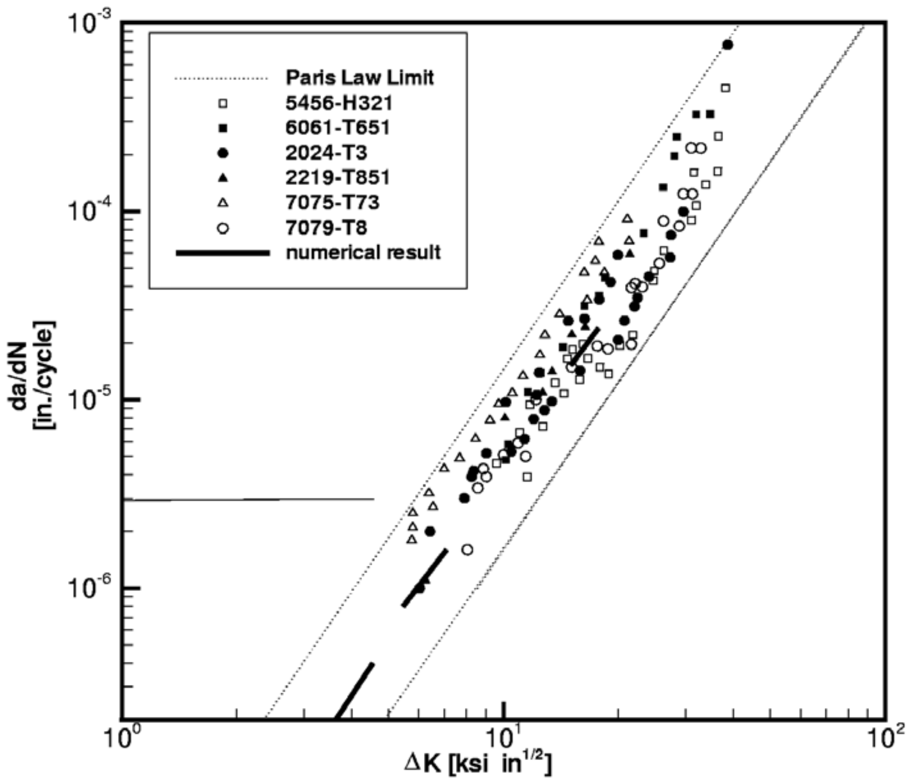

Comparison of computed and experimental growth rates.
Initial crack lengths = 10, 20 and 30 mm
(Data from ASTM Standards, Vol. 3.2, 1991)

(Nguyen, Repetto and Ortiz, 2000)

Michael
Ortiz

Fatigue crack growth - Short cracks

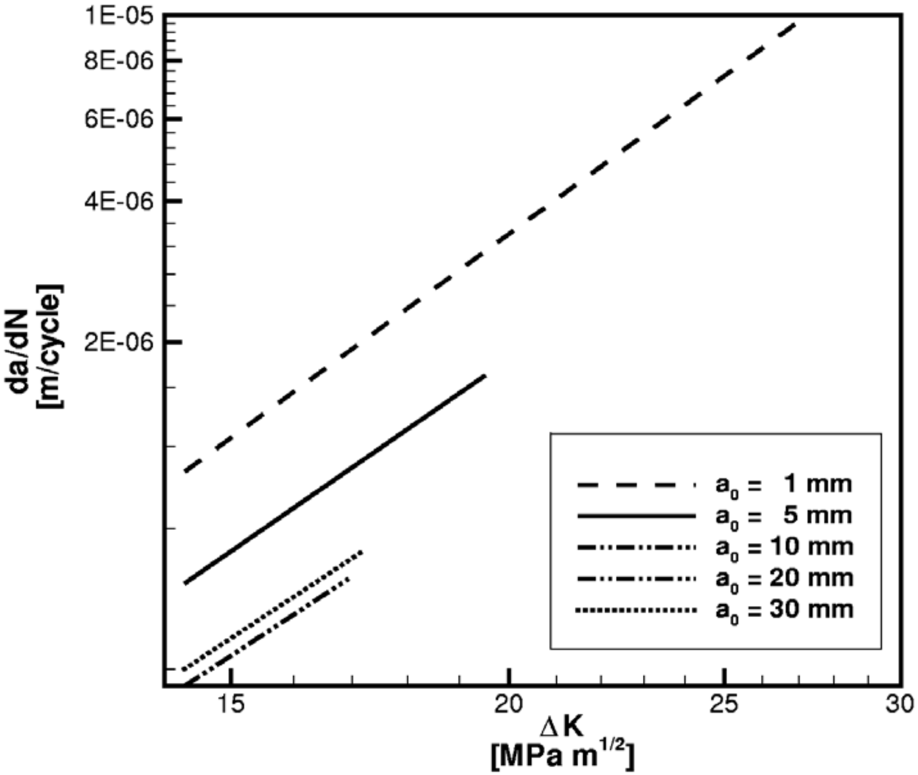

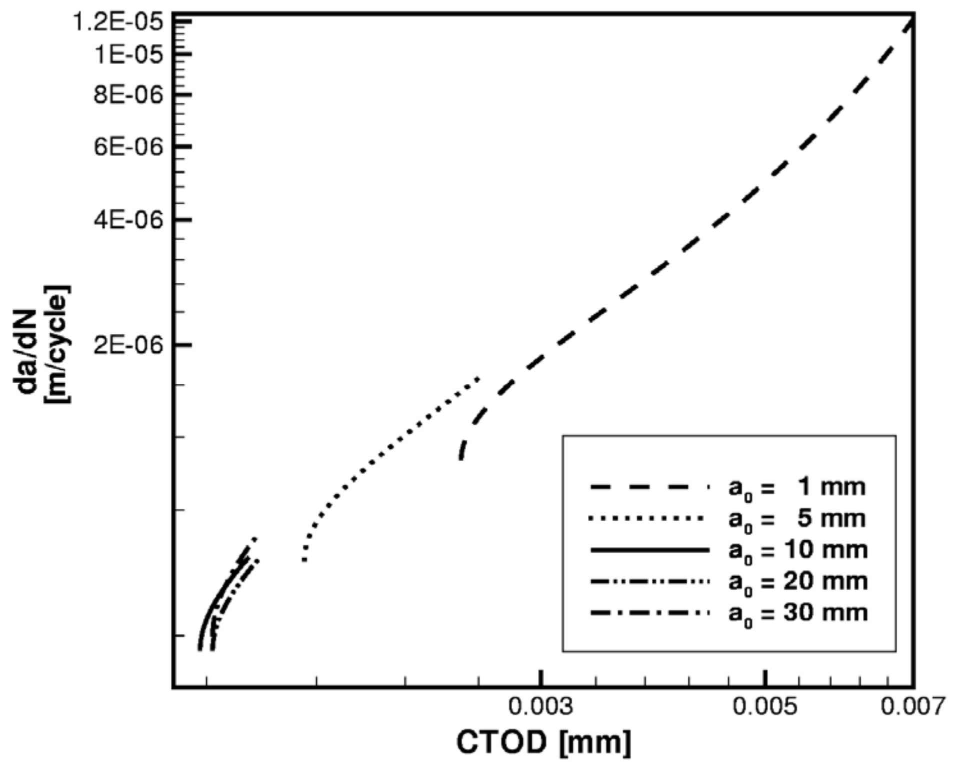

- Modified Paris law: $$\frac{da}{dN} = C(\Delta\delta)^n = C'(\Delta J)^n$$

(Dowling, 1977; Kanninen et al., 1981)

Michael Ortiz

Fatigue crack growth - Overload effect

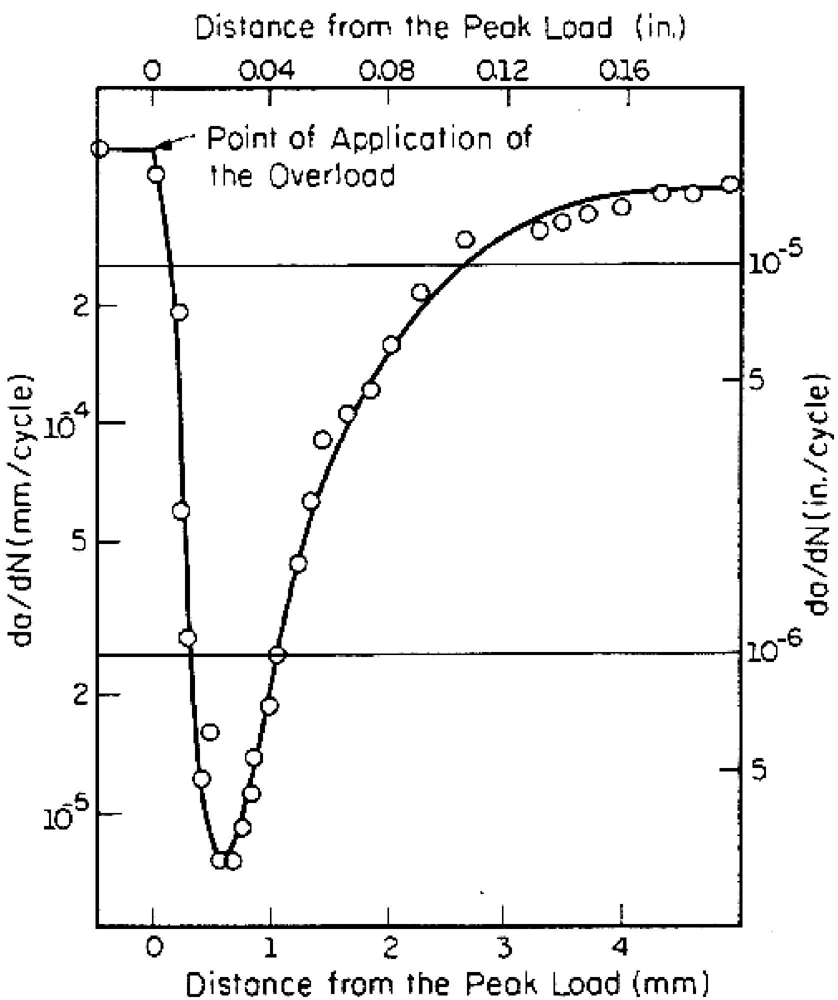

(Von Euw et al., ASTM STP 513, 1972)

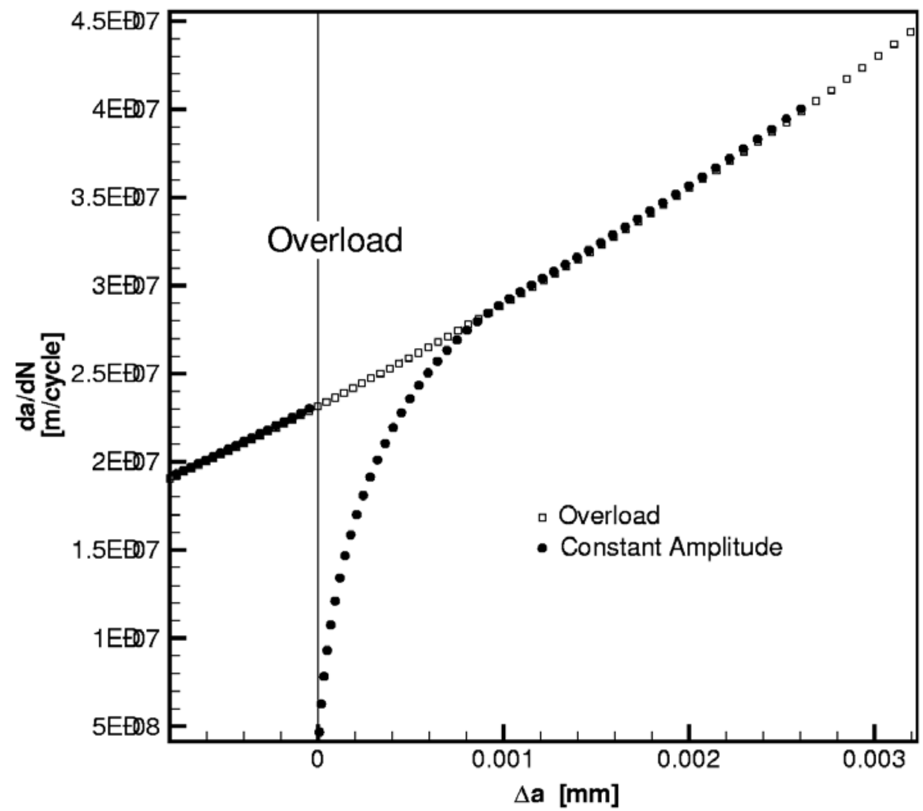

Effect of single 50% overload on growth rate.
Initial crack length = 10 mm.
(Nguyen, Repetto and Ortiz, 2000)

Michael
Ortiz

Issues for further study

- Crack nucleation
- Crack patterns in the presence of profuse branching, fragmentation:
  - *Geometry of crack ensemble (fractal dimension?)*
  - *Energy balance, dissipation*
  - *Convergence of finite-element solutions*
- Disparity between atomistic and continuum cohesive strengths, critical opening displacements.
- Multiscale modeling:
  - *Cohesive models and discrete dislocation models*
  - *Chemistry, impurity diffusion*
- Transonic cracks

Stress corrosion cracking

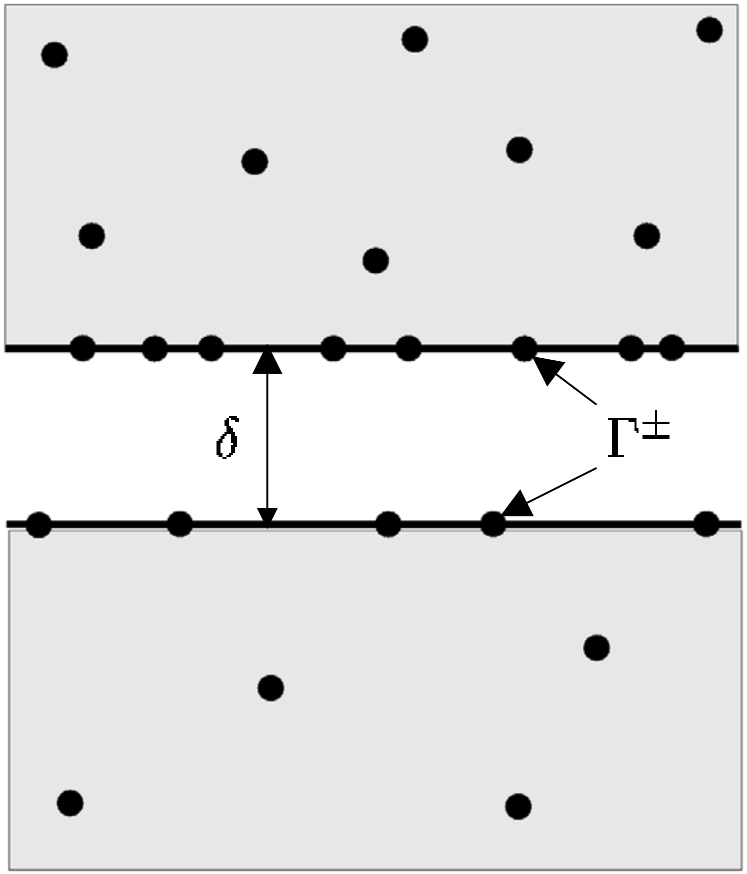

- Cohesive free energy density:

$$F = F(\delta, \Gamma^{\pm})$$

- Limiting values:

$$\lim_{\delta \to \infty} F(\delta, \Gamma^{\pm}) = \gamma_s(\Gamma^{+}) + \gamma_s(\Gamma^{-})$$

$$\lim_{\delta \to 0} F(\delta, \Gamma^{\pm}) = \gamma_b(\Gamma^{+} + \Gamma^{-})$$

- Equilibrium with environment:

$$\frac{\partial F}{\partial \Gamma^{\pm}}(\delta, \Gamma^{\pm}) = \mu^{\text{env}}$$

Michael Ortiz

Stress corrosion cracking

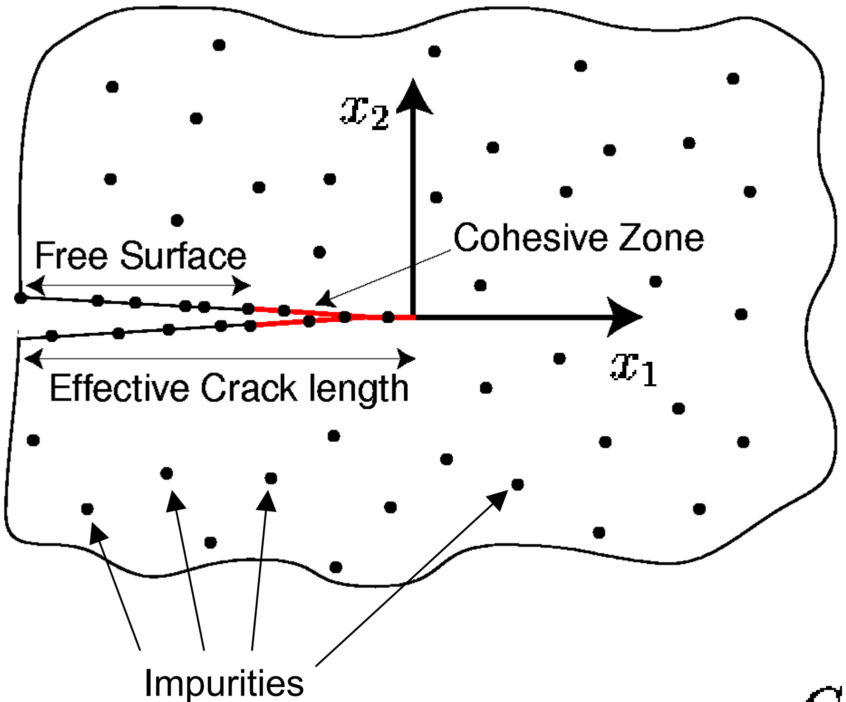

- Diffusion equation:

$$C_{,t} + \nabla \cdot \mathbf{J} = 0$$

- Impurity flux: $\mathbf{J} = -M\, C\, \nabla \mu$
- Chemical potential:

$$\mu = G + RT\, \log(\gamma V_m C) + E$$

- Elastic energy: $E = p \Delta V$
- Diffusion equation:

$$C_{,t} = D \nabla^2 C + (M\, \Delta V)\, \nabla \cdot (C\, \nabla p)$$

- Equilibrium at crack flanks: $\mu = \frac{\partial F}{\partial \Gamma^{\pm}}(\delta, \Gamma^{\pm}), \quad x_2 = 0^{\pm}$

Michael Ortiz

Stress corrosion cracking

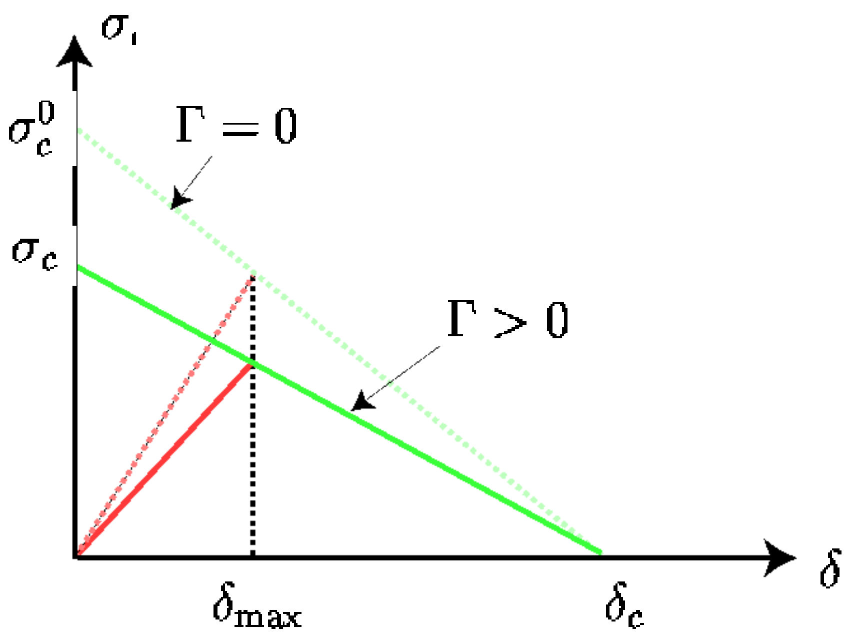

- Segregant embrittlement: (Wang and Rice, 1989):

$$2\gamma_s(\Gamma) = 2\gamma_s^0 - (\Delta g_b^0 - \Delta g_s^0)\,\Gamma$$

- Effect on cohesive law:

$$\sigma_c(\Gamma) = \sigma_c^0 - \frac{(\Delta g_b^0 - \Delta g_s^0)}{\delta_c}(\Gamma^+ + \Gamma^-)$$

Impurity	$-\Delta g_s^0$	$-\Delta g_b^0$	$\Delta g_b^0 - \Delta g_s^0$
C	73 to 85	50 to 75	-2 to 35
P	76 to 80	32 to 41	35 to 48
Sb	83 to 130	8 to 25	58 to 122
S	165 to 190	50 to 58	107 to 140

(Steel, 300K, g in KJ/mol; after Wang and Rice, 1989)

Michael Ortiz

Case study: Hydrogen embrittlement

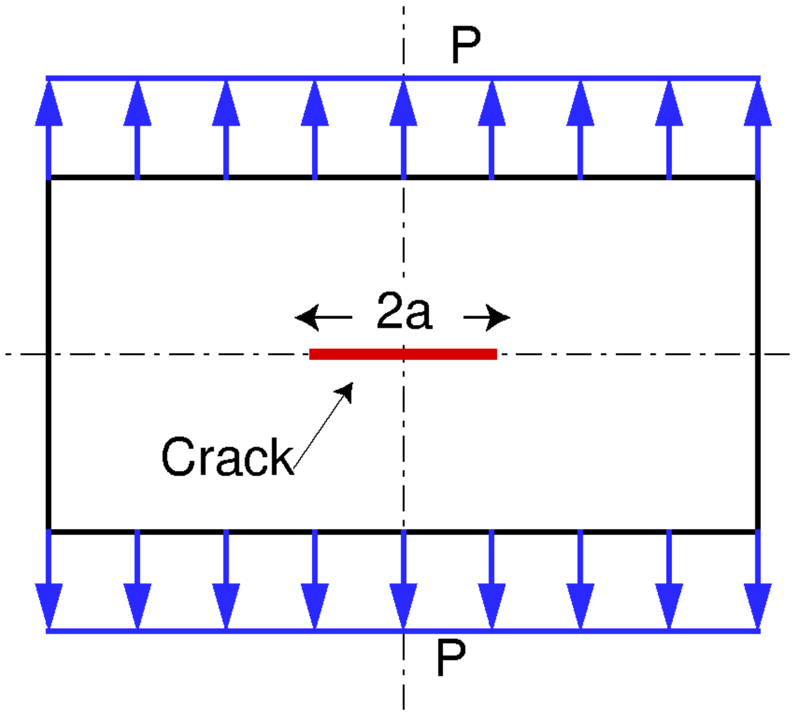

Center-crack panel geometry.
Initial crack length = 0.25 mm.
Applied stress = 260 MPa.

- Material properties (H, steel):

E	207 GPa
ν	0.3
G_c	1,260 J/m^2
σ_c	840 MPa
δ_c	3×10^{-6} m
D	1.27×10^{-8} m^2/s
V_m	7.116×10^{-6} m^3/mol
ΔV	2×10^{-6} m^3/mol
C_0	2.084×10^{21} m^{-3}

Michael
Ortiz

Case study: Hydrogen embrittlement

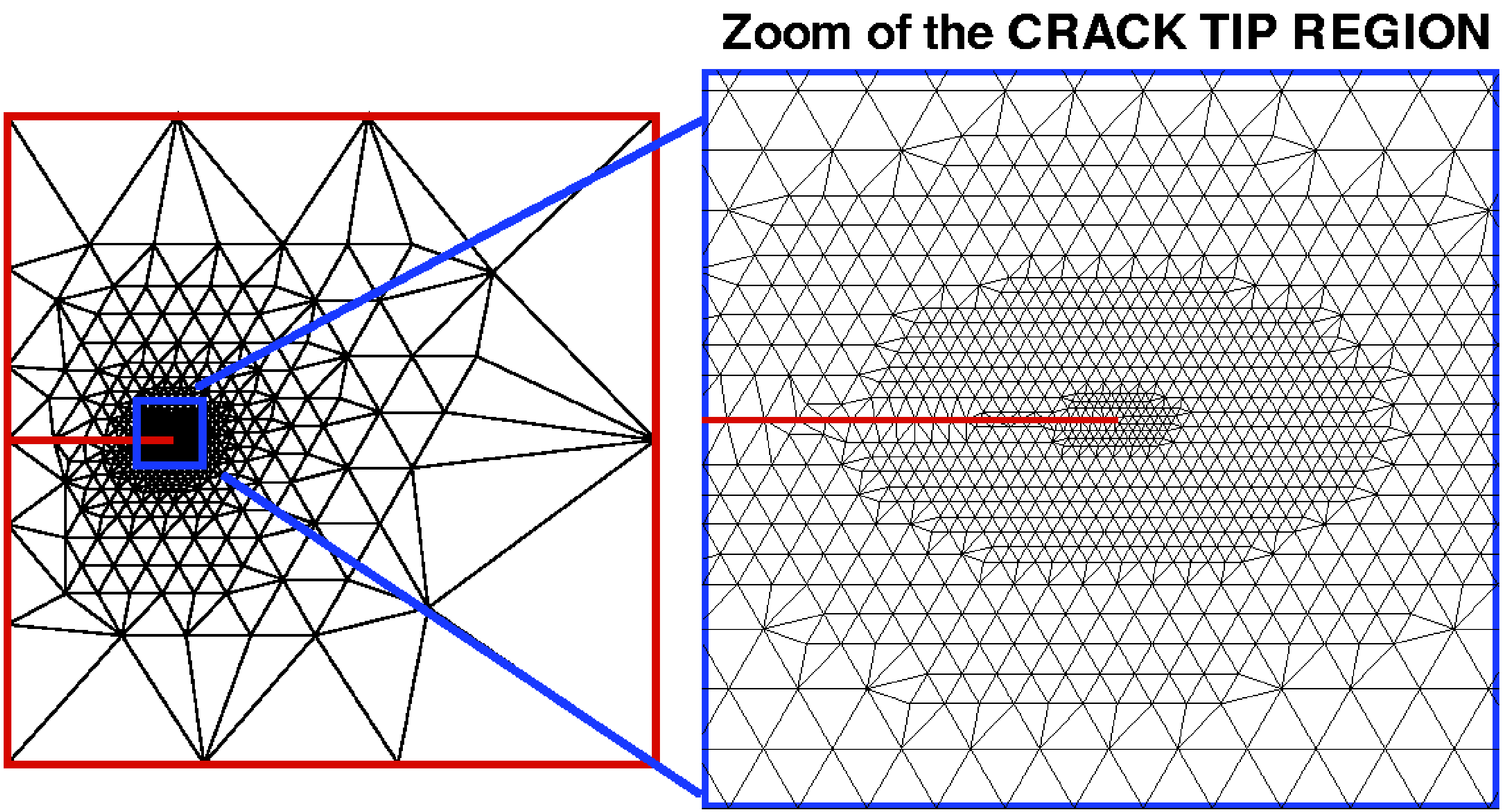

Initial mesh

Michael
Ortiz

Case study: Hydrogen embrittlement

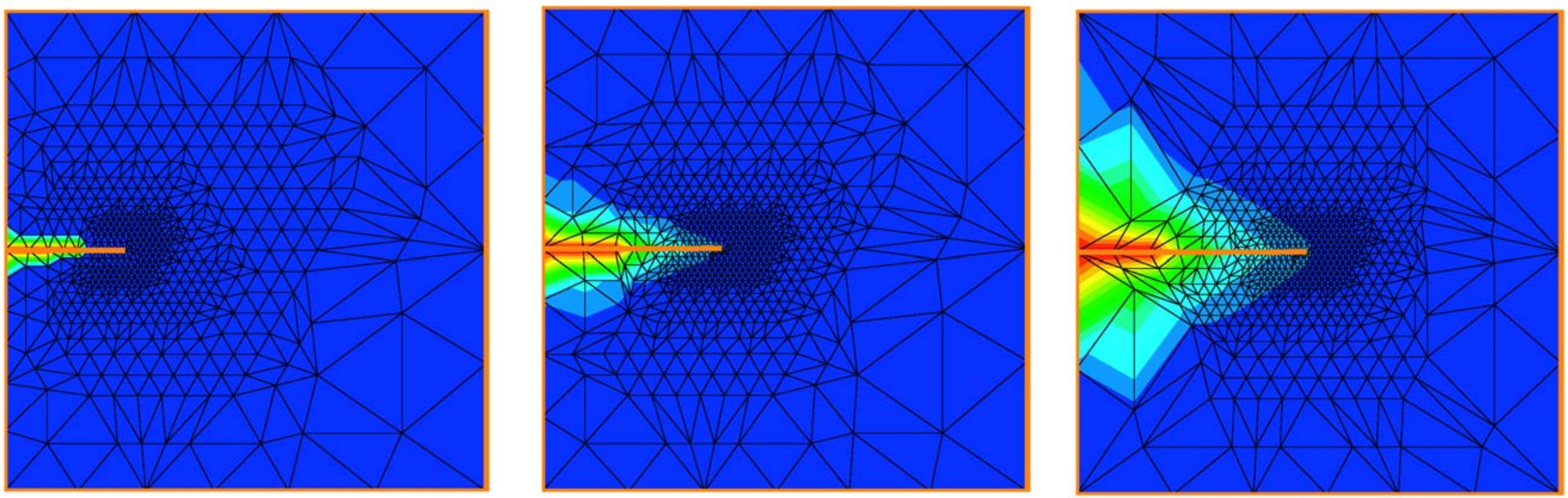

Evolution of
hydrogen concentration

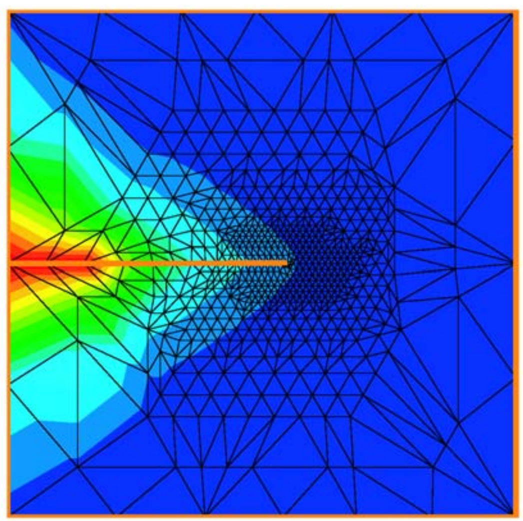

(Movie)

Michael
Ortiz

Condensed matter quantum chemistry

(Courtesy of Emily Carter)

- Challenges:
  - *High dimensionality*
  - *Singular, long-range interaction potentials*
  - *Breadth of length & time scales*
- Ultimate Impact:
  - *Efficient & accurate simulations of complex chemistry*
  - *Mapping to macro-scopic mechanics*

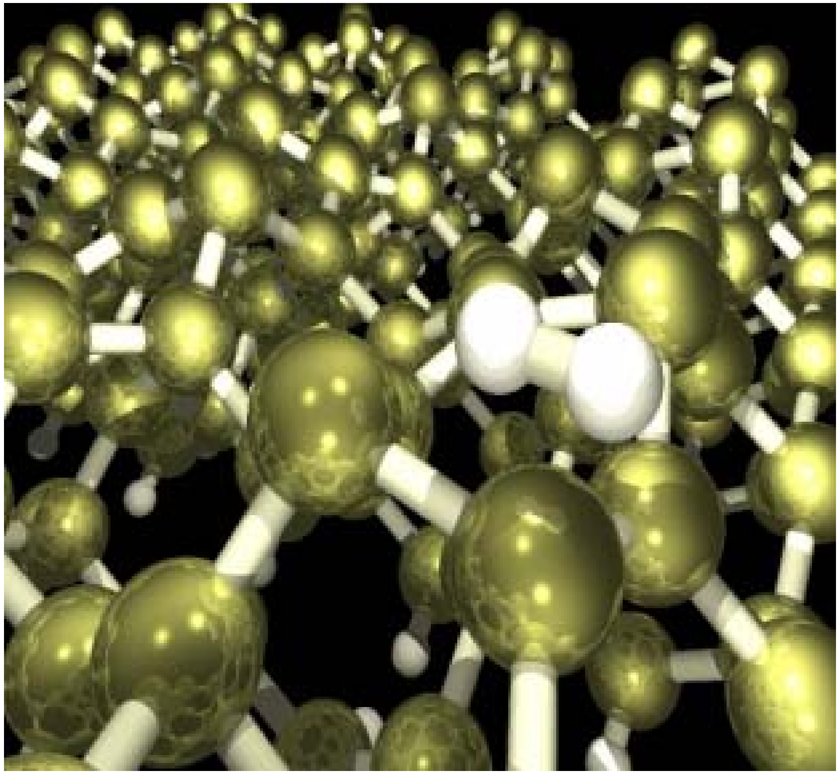

Adsorption of H molecule by Si surface.
(Radehe and Carter, Ann. Rev. Phys. Chem., 1997)

Michael
Ortiz

Issues for further study

- Crack nucleation
- Crack patterns in the presence of profuse branching, fragmentation:
  - *Geometry of crack ensemble (fractal dimension?)*
  - *Energy balance, dissipation*
  - *Convergence of finite-element solutions*
- Disparity between atomistic and continuum cohesive strengths, critical opening displacements.
- Multiscale modeling:
  - *Cohesive models and discrete dislocation models*
  - *Chemistry, impurity diffusion*
- Transonic cracks